Redox Biology 84 (2025) 103696

Contents lists available at ScienceDirect

Redox Biology

journal homepage: www.elsevier.com/locate/redox

Histones in neutrophil extracellular traps (NETs) contain oxidative post-translational modifications induced by the myeloperoxidase oxidant hypochlorous acid

Helen Hemmling, Line A.E. Hallberg, Per Hägglund *, Clare L. Hawkins **

Department of Biomedical Sciences, University of Copenhagen, Panum, Blegdamsvej 3B, Copenhagen N, DK-2200, Denmark

ARTICLE INFO

Keywords:
Neutrophil
Hypochlorous acid
Post-translational modification
3-Chlorotyrosine
Inflammation

ABSTRACT

Extracellular traps (NETs) released by neutrophils during inflammation play a role in clearing infection but also contribute to disease pathology. NETs consist of a DNA backbone containing histones, anti-microbial granule proteins, such as myeloperoxidase (MPO), and other proteins. MPO remains enzymatically active and generates hypochlorous acid (HOCl) to kill pathogens. However, HOCl also readily reacts with proteins, but whether histones and other NET proteins are modified by this oxidant is unknown. This is significant as post-translational modification of histones alters their intracellular and extracellular reactivity. In this study, we used a proteomic approach to characterise the protein composition of NETs and identify HOCl-induced oxidative modifications on histones and other proteins. NETs were collected from primary neutrophils and the PLB-985 cell line and stimulated with phorbol myristate acetate (PMA) or nigericin, a bacterial peptide derived from *Streptomyces hygroscopicus*. There was evidence for Lys nitrile and aminoadipic semialdehyde formation, Tyr and Trp chlorination, and Met oxidation on histones and other proteins, including quinone oxidoreductase. Chlorination of Tyr-88 on histone H4 was particularly abundant and occurred to a greater extent in NETs from neutrophils exposed to PMA compared to nigericin, consistent with nigericin triggering NET release via a non-oxidative pathway. Chlorination of histone H4 Tyr-88 was also observed in the nuclear and cytoplasmic cell extracts of stimulated cells and could be decreased on treatment of the neutrophils with the MPO inhibitor AZD5904. These findings provide the first evidence that HOCl modifies proteins within NETs, particularly histone H4, which may be relevant in disease.

1. Introduction

Extracellular traps (ETs) are released by neutrophils and other immune cells during inflammatory processes [1] and play a key role in pathology [2]. There is growing evidence that ETs, particularly those released by neutrophils (NETs), are involved in the development of disease, including atherosclerosis [3], sepsis [4] and COVID-19 [5], in addition to their innate immune function of clearing infection [2]. In general, ETs are composed of a mesh of DNA, histones and various other proteins, the composition of which can be dependent on the cell type and stimulus [6,7]. Proteomic studies have identified more than 150 different NET-associated proteins, derived from cells, or from the circulation [8–11], with many of these cell-derived proteins also identified in ETs from macrophages (METs) [12]. The pathways responsible for the release of NETs, known as NETosis, have been characterised in detail (reviewed [2,7,13]).

NETosis can be broadly divided into two different types, which are either dependent or independent of the activation of NADPH oxidase 2 (NOX2) [2]. In NOX2-dependent NET release, various triggers such as pathogens and lipopolysaccharides (LPS), or inflammatory mediators such as tumour necrosis factor α (TNFα), and phorbol myristate acetate (PMA), activate protein kinase C (PKC) [7]. This induces the assembly of NOX2 resulting in the formation of superoxide ($O_2^{\bullet-}$) [6], which can dismutate to hydrogen peroxide (H_2O_2) [14]. Hydrogen peroxide can then be utilised together with chloride ions by myeloperoxidase (MPO) to form hypochlorous acid (HOCl) [15], which can also be a trigger of NET release [16,17]. PKC induces alterations in intracellular Ca^{2+} levels [6], which activates peptidyl arginine deiminase 4 (PAD4) [6,18]. This results in citrullination of histone Arg residues and decondensation of

* Corresponding author.
** Corresponding author.
E-mail addresses: pmh@sund.ku.dk (P. Hägglund), clare.hawkins@sund.ku.dk (C.L. Hawkins).

https://doi.org/10.1016/j.redox.2025.103696
Received 29 April 2025; Received in revised form 20 May 2025; Accepted 20 May 2025
Available online 23 May 2025
2213-2317/© 2025 The Authors. Published by Elsevier B.V. This is an open access article under the CC BY-NC license (http://creativecommons.org/licenses/by-nc/4.0/).

Abbreviations

ACN	acetonitrile
ATRA	all-trans retinoic acid
BSA	bovine serum albumin
Cl-Tyr	3-chloro-Tyr
DDA	data-dependent acquisition
DIA	data-independent acquisition
diCl-Tyr	3,5-dichloro-Tyr
DMSO	dimethyl sulfoxide
DTT	dithiothreitol
ETs	extracellular traps
FA	formic acid
FBS	fetal bovine serum
H_2O_2	hydrogen peroxide
HBSS	Hank's balanced salt solution
HOCl	hypochlorous acid
IAM	iodoacetamide
LPS	lipopolysaccharide
MET	macrophage extracellular trap
MPO	myeloperoxidase
mtDNA	mitochondrial DNA
NET	neutrophil extracellular trap
NOX2	NADPH oxidase complex 2
NQO1	NAD(P)H quinone oxidoreductase 1
$O_2^{\bullet-}$	superoxide
PAD4	peptidyl arginine deiminase 4
PKC	protein kinase C
PMA	phorbol myristate acetate
PPP	pentose phosphate pathway
PTMs	post-translational modifications
RA	rheumatoid arthritis
ROS	reactive oxygen species
RPMI-1640	Roswell Park Memorial Institute 1640 medium
SASA	solvent accessible surface area
SEM	standard error of the mean
SLE	systemic lupus erythematosus
TFA	trifluoroacetic acid
TNFα	tumour necrosis factor α

heterochromatin, which facilitates NET release [2,19]. Anti-microbial granular proteins associate to the decondensed chromatin network after disintegration of the nuclear membrane, which is followed by the release of NETs into the extracellular environment [20]. NOX-independent NET release can be triggered by a range of other stimuli, particularly ionophores, such as the bacterial toxin nigericin from *Streptomyces hygroscopicus* and ionomycin, which induce the efflux of mitochondrial K^+ or facilitate Ca^{2+} transport, respectively, to promote the influx of Ca^{2+} and activation of PAD4 [7,21]. This NETosis pathway occurs independently of oxidant formation, but can still involve PAD4 activation, owing to the influx of Ca^{2+} [21].

While the protein composition of NETs can be dependent on the stimulus [22], typically, the most abundant NET-associated proteins are different types of histones, MPO, neutrophil elastase, catalase, α-enolase, transketolase and various antimicrobial proteins such as lactotransferrin, myosin-9, plastin-2 and lysozyme C [8–11]. The core histones (H2A, H2B, H3 and H4) are more abundant in NETs then the linker histone H1 [8]. Histones are small alkaline proteins, that play a crucial role in transcriptional regulation [23]. This is related to various post-translational modifications (PTMs) that alter the ability of the histones to bind to DNA [24,25]. The abundance of Lys and Arg residues within histones means that these proteins are very susceptible to PTMs, which can also be considered as epigenetic marks [24]. Common PTMs of histones include methylation of Arg and Lys, acetylation of Lys, phosphorylation of Ser, Thr and Tyr and ubiquination of Lys [26–28]. The Arg residues on histones in NETs can also be citrullinated [2,7,19,29].

In addition to enzymatic PTMs, histones can be modified by oxidants, including HOCl, which may also be relevant in vivo [30,31]. Exposure of histones to HOCl results in the formation of different products, including unstable *N*-chloramines, which can decompose to form nitriles or aminoadipic semialdehydes on Lys residues [30,32]. The reaction of HOCl with Tyr to form 3-chloro-Tyr (Cl-Tyr) and 3,5-dichloro-Tyr (diCl-Tyr) is also reported on histones and occurs readily on core histones H2A, H2B and H4, which possess a YXXK/KXXY sequence motif, shown to be a preferred chlorination site [30,31]. Histones are likely to be favourable targets for HOCl under pathological conditions since catalytically-active MPO and histones are both localised on the backbone of NETs [33]. Recent studies have shown that modification of histones by HOCl can influence their reactivity in the extracellular environment where they are cytotoxic and can promote inflammation [34]. However, overall, it is not well understood how the PTMs of histones affects their extracellular reactivity [34–36].

The hypothesis for this study is that histones and other proteins localised on the DNA backbone of NETs will contain oxidative PTMs, as a result of exposure to HOCl formed by MPO. We performed proteomic analyses to identify HOCl-induced protein modifications, focusing primarily on histones, owing to their high abundance in NETs. Experiments were performed with primary neutrophils and the neutrophilic PLB-985 cell line exposed to model inflammatory (PMA) and pathogenic (nigericin) stimuli. Evidence was obtained for the modification of histone Lys, Tyr and Met residues, on NETs released from each type of neutrophil, particularly on stimulation of the cells with PMA. In addition to histones, oxidative modifications were also observed on other proteins, including quinone oxidoreductase, myosin-10 and transaldolase. Overall, these data show novel HOCl-induced oxidative post-translational modifications on extracellular histones present in NETs, which could be relevant in inflammatory pathologies.

2. Materials and methods

2.1. Reagents and materials

All aqueous solutions were prepared using nanopure H_2O from a MilliQ system (Millipore; Merck, Darmstadt, Germany). All chemicals and reagents were of the highest purity available and purchased from VWR (Søborg, Denmark) unless stated otherwise. The concentration of HOCl was determined by UV absorbance at 292 nm at pH 11 using an extinction coefficient of 350 M^{-1} cm^{-1} [37].

2.2. Culturing, differentiation and treatment of PLB-985 cells

PLB-985 cells (human acute myeloid leukaemia cells, ACC 139, Leibniz Institute DSMZ, Braunschweig, Germany) were cultured in Roswell Park Memorial Institute 1640 medium containing glutamine (RPMI-1640; Gibco, from Thermo Fisher, Waltham, MA, USA) supplemented with 10 % fetal bovine serum (FBS; Gibco) and 1 % penicillin/streptomycin (100 U/mL; Gibco). Cultivation was performed at 37 °C and 5 % CO_2. Every 2–3 days the cells were passaged and reseeded with a cell density of 0.2×10^6 to 1.5×10^6 cells/mL. For differentiation, the PLB-985 cells were seeded at a density of 0.3×10^6 cells/mL in culture medium supplemented with all-trans retinoic acid (ATRA, 2 μM; Sigma-Aldrich, St. Louis, MO, USA) and dimethyl sulfoxide (DMSO, 1.3 %; Sigma-Aldrich) for 72 h [38,39]. After differentiation, cells were counted, centrifuged (125×*g* for 5 min at 21 °C) and resuspended in RPMI-1640 medium supplemented with glutamine (2 mM; Gibco) but

without phenol red. To induce NET formation, 10 mL of 1 × 10^6 cells/mL were seeded in a T75 flask and treated for 4 h with nigericin (15 μM; J61349, Thermo Fisher) or PMA (50 nM; P8139, Sigma-Aldrich), as previously, where NET release was visualised by fluorescence microscopy using Sytox green and quantified by the Quant-iT™ PicoGreen™ dsDNA assay kit [38]. For the mass spectrometry analysis of PLB-985 cells without stimulation or with stimulation with nigericin (15 μM) in the absence or presence of an MPO-inhibitor, the cells were seeded as described before and an MPO-inhibitor (10 μM, AZD5904; MedChemExpress, from Nordic Biosite, Copenhagen, Denmark) was added 15 min before adding nigericin. Stock solutions of nigericin (10 mM), PMA (2 mM) and MPO inhibitor (500 μM) were prepared in DMSO and were sterile filtered before dilution into RPMI-1640 medium and addition to the cells.

2.3. Primary neutrophils isolation and NET collection

Freshly isolated buffy coats from anonymous donors were obtained from a blood bank (Rigshospitalet, Copenhagen, Denmark) on the same day as the experiments. The collected buffy coat was diluted 1:4 with pre-warmed Hank's balanced salt solution (HBSS, Gibco) at 37 °C. The buffy coat was layered onto a Ficoll-Paque™ PLUS 1:1.3 (Cytvia, Vallensbæk Strand, Denmark) gradient, using a ratio of 3 parts Ficoll to 4 parts buffy coat mixture. The granulocytes and erythrocytes were isolated by centrifugation (400×*g* for 30 min at 21 °C) and transferred to a new tube. The cell pellet was immediately resuspended in 3 vol of PBS and 1 volume of 4 % dextran with incubation for 30 min at 21 °C to remove erythrocytes. The supernatant, which contains the neutrophils, was collected and centrifuged (250×*g* for 5 min at 21 °C). After centrifugation, the cell pellet containing the neutrophils was resuspended in 5 mL of red cell lysis buffer (Roche, Cat. No. 11,814,389,001, from Merck) for 10 min. The neutrophils were isolated by centrifugation (250×*g* for 5 min at 21 °C) and washed with pre-warmed HBSS at 37 °C until the supernatant was colourless. To induce NET formation, the primary neutrophils (cell density: 1 × 10^6 cells/mL) were suspended in RPMI-1640 medium supplemented with glutamine (2 mM) but without phenol red and treated for 3 h with either nigericin (15 μM) or PMA (50 nM) as previously, where NET release was visualised by fluorescence microscopy using Sytox green and quantified by the Quant-iT™ PicoGreen™ dsDNA assay kit [7,38].

2.4. Quantification of HOCl production in PLB-985 cells using R19-S

The PLB-985 cells were cultured and differentiated as described above. After differentiation, the cells were washed twice with HBSS before addition of R19-S (10 μM, L8001-AHJU1911, FutureChem Co., Seoul, Korea) to the PLB-985 cells (2.2 × 10^6 cells/mL) and incubation for 10 min, as described previously [38,40]. The MPO-inhibitor (1–10 μM; AZD5904, MedChemExpress from Nordic Biosite, Copenhagen, Denmark) was added to the cells immediately before stimulation with 50 nM PMA. The samples were transferred to a 96 well black tissue culture plate (Greiner, Kremsmünster, Austria) and incubated at 37 °C for a total of 4 h while measuring the fluorescence at λ_{ex} 515 nm and λ_{em} 550 nm every 30 min using a SpectraMax® i3x plate reader (Molecular Devices, San Jose, CA, USA). The concentration of HOCl was determined from a standard curve. Stock solutions of R19-S (250 μM) were prepared in acetonitrile (ACN).

2.5. Preparation and quantification of proteins for mass spectrometric analysis

The NETs were removed from the stimulated neutrophils and PLB-985 cells by the addition of 10 μL DNase I (40 U/μL, D2821-10KU, Sigma-Aldrich) dissolved in 20 mM Tris HCl, 1 mM magnesium chloride and 50 % v/v glycerol, in accord with previous studies [8,38]. Following incubation (10 min), 5 mM EDTA (Sigma-Aldrich) was added to inactivate DNase I. To remove the cells, the samples were centrifuged (300×*g* for 5 min at 21 °C) and the supernatant containing NETs was transferred to a new tube. The samples were again centrifuged (1600×*g* for 5 min at 21 °C) to remove cell debris and supernatants were transferred to Vivaspin 6 ultrafiltration devices (MWCO: 10 kDa; Sartorius Stedim Lab Ltd, from VWR) and concentrated by centrifugation (4000×*g* for 4–20 min at 21 °C). The cell pellet was washed once with PBS and centrifuged (500×*g* for 2–3 min at 21 °C). After removing the PBS, the cells were either added to a lysis buffer (8 M urea in 100 mM Tris buffer at pH 8.5) or were used to prepare nuclear extracts using the NE-PER™ Nuclear and Cytoplasmic Extraction Kit from Thermo Fisher Scientific (cat. no.: 78833) following the manufacturer's instructions.

Briefly, for each 20 μL cell pellet, 200 μL CER I buffer, 11 μL CER II buffer and 100 μL NER buffer was used, with all incubation and centrifugation steps performed on ice or at 4 °C. Ice-cold CER I was added to the cell pellet, vortexed for 15 s to fully lyse the pellet and incubated for 10 min on ice. Then, ice-cold CER II was added, vortexed for 5 s and incubated for 1 min on ice. The tube was vortexed again for 5 s and centrifuged (16,000×*g* for 5 min). The supernatant containing the cytoplasmic fraction was immediately transferred to a fresh tube and was stored on ice until use. The pellet which contains the nuclei was resuspended in ice-cold NER, vortexed 15 s and incubated for 10 min on ice. Cycles of vortexing and incubation on ice were repeated for a total of 40 min. Finally, the tube was centrifuged (16,000×*g* for 10 min) and the supernatant containing the nuclear extract was transferred to a fresh tube and placed on ice until use. To stop protein degradation in the samples, all sample buffers were supplemented with protease inhibitors (1 %; P8340-5 ML, Sigma-Aldrich).

A Bradford assay was used to determine the protein concentration in the samples. The Bradford reagent was prepared by diluting the Bio-Rad® protein assay reagent 1:5 in Milli-Q water (Millipore, Merck). 10 μL of the sample was added to 200 μL of diluted Bradford reagent in a clear 96 well tissue culture plate (VWR) and incubated for 5 min at 21 °C. The absorbance was measured at 595 nm with a SpectraMax® i3x plate reader (Molecular Devices) and protein concentration determined based on a standard curve prepared with bovine serum albumin (BSA).

2.6. Proteolytic digestion

Proteins were enzymatically digested using an SP3-based approach, as previously described [41]. Samples containing 20 μg protein were added to a solution of 8 M urea in 100 mM Tris, pH 8.5 (Sigma-Aldrich; total volume of sample with buffer 200 μL) that had been pre-degassed with nitrogen for 30 min to reduce artifactual oxidation. 5 mM dithiothreitol (DTT; Sigma-Aldrich) was added, with incubation for 30 min at 21 °C, followed by addition of 5 mM iodoacetamide (IAM; Sigma-Aldrich) and incubation for 30 min at 21 °C in the dark. Samples (220 μL) were mixed with an equal volume of ethanol (Sigma-Aldrich), and added in a 1:55 ratio of magnetic bead solution of two different Sera-Mag Magnetic Carboxylate Modified Particles (Cytiva, lot: 44152105050250 and 24152105050250), with incubation for 30 min in a thermomixer at 24 °C and with a speed of 1000 rpm. Next, samples were placed on a magnet and the supernatant was carefully removed. Then 80 % v/v ethanol was added, mixed carefully with the beads, and the tubes were placed on magnet again to enable removal of the supernatant. This step was repeated twice before removing the magnet and adding 100 μL trypsin digestion buffer (100 mM Tris buffer, pH 8) and 1 μL trypsin (0.1 μg/μL; Promega, V5111A), followed by overnight incubation at 21 °C. Stock solutions of trypsin (0.1 μg/μL) were prepared in 10 mM hydrochloric acid (HCl) and stored at −20 °C.

Proteolytic peptides were isolated by a stage tipping approach based on Rappsilber et al. [42]. Filter AttractSPE™ Disks Bio - C18 (AFFINISEP, Le Houlme, France) were activated with 100 % methanol or acetonitrile, then conditioned with 80 % v/v ACN containing 0.1 % v/v trifluoroacetic acid (TFA; Sigma-Aldrich) before equilibration with 0.1 % v/v TFA. Between these steps, the filter tips with tubes were

centrifuged at 21 °C (1200×*g* for 1 min). The digested samples were acidified with 10 % v/v TFA to reach a pH < 2 and were loaded to the activated filter tips which were then centrifuged again (1200×*g* for 3 min). The filters with the peptides were washed twice with 0.1 % v/v TFA with centrifugation between washing steps (1200×*g* for 1 min). The peptides were eluted with 80 % v/v ACN containing, 0.1 % v/v formic acid (FA), and the samples were centrifuged (1200×*g* for 1 min) into fresh tubes. Finally, samples were dried using a Speedvac (Refrigerated Condensation Trap RT490, SAVANT, from Thermo Fisher). Prior to MS analysis, samples were reconstituted in 20 μL 0.1 % v/v formic acid to final concentration of 1 μg/μL digested protein.

2.7. Mass spectrometry analysis

Samples were analysed on a Bruker TIMS TOF PRO mass spectrometer (Bruker Daltonics, Bremen, Germany) in the positive ion mode with a Captive spray ion source on-line connected to a Dionex Ultimate 3000RSnano chromatography system (Thermo Fisher Scientific). Peptides corresponding to 1 μg of digested protein were separated on an Aurora column (C18, 1.7 μM, 25 cm, 75 μm ID; Ion optics) at 60 °C with a solvent gradient of 0.1 % v/v FA (Solvent A) and 99.9 % v/v ACN/0.1 % v/v formic acid (Solvent B) over 42 min or 140 min, at a flow rate of 400 nL min^{-1}. For the experiments with the MPO inhibitor, peptides were separated as above, but with a 15 cm Aurora column and 22 or 28 min gradients at 35–45 °C. The mass spectrometer was operated in either DIA or DDA PASEF mode with 1.1 s cycle time and TIMS ramp time of 100 m s. MS scan range was set to 100–1700 *m/z*. Protein abundance was calculated from DIA data based on MaxLFQ output values from database searches in DIA-NN (version 1.8.2 beta11) using a spectral library generated *in silico* with the following parameters: trypsin with 1 missed cleavage; cysteine carbamidomethylation (fixed modification), methionine oxidation and N-terminal acetylation (variable modifications); peptide charge: 2–4; peptide length: 7–25); precursor FDR: 1 %. Modified peptides were identified from DDA data using FragPipe (versions 20.0 and 21.1), with the following parameters: 2 missed tryptic cleavages; 20 ppm parent and fragment mass tolerance; 1 % FDR, fixed modification: IAM alkylation of Cys (+57.02146 Da), variable modifications: Met oxidation (+15.9949 Da), nitrile formation on Lys (−4.0313 Da), chlorination of Tyr and Trp (+33.96103 Da), semialdehyde formation on Lys (−1.031634 Da), acetylation of Lys (+42.0106 Da) and citrullination/deamidation on Arg and Asn (+0.9840 Da), respectively. Perseus (version 1.6.15.0) was used for post-processing and filtering of data. GraphPad Prism (version 10.2.0) was used for generation of pie charts, volcano plots and bar graphs. Validation of identified modified peptides based on idotp values and calculation of occupancy for chlorinated peptides was performed using Skyline (23.1.0.168). Occupancy of the chlorination site Tyr-88 in Histone H4 is defined as the sum of the total peak area of the specific precursor ions (MS1) with combination of different charge states corresponding to the chlorinated peptide (TVTAMDVVY[Cl]ALK, TVTAM[ox]DVVY[Cl]ALK, TVTAMDVVY[Cl]ALKR and TVTAM[ox]DVVY[Cl]ALKR), divided by the sum of the total peak area of all identified peptides (both chlorinated at Tyr-88 and non-chlorinated: TVTAMDVVY[Cl]ALK, TVTAM[ox]DVVY[Cl]ALK, TVTAMDVVY[Cl]ALKR and TVTAM[ox]DVVY[Cl]ALKR, TVTAMDVVYALK, TVTAM[ox]DVVYALK, TVTAMDVVYALKR and TVTAM[ox]DVVYALKR).

2.8. Statistical analyses

All experiments are representative of at least 3 independent experiments with mean ± standard error of mean (SEM). GraphPad Prism version 10.2.0 was used to perform different statistical analyses as indicated in the figure legends. Unpaired t-tests, one-way ANOVA or two-way ANOVA were used to determine significance ($P < 0.05$) with details of the specific post-hoc tests given in the Figure Legends.

3. Results

3.1. NETs released from primary neutrophils and PLB-985 cells exposed to nigericin and PMA display different protein compositions

NETs released from primary neutrophils and PLB-985 cells following exposure to PMA and nigericin were subjected to LC-MS based proteomics analysis. The conditions used to stimulate NET release and collect the NET proteins were based on previous studies, where extracellular DNA was visualised and quantified using the fluorescent stains Sytox green and PicoGreen, respectively [38]. In general, a much larger number of proteins were identified in the NETs from the primary neutrophils compared to PLB-985 cells, although the same amount of digested protein (1 μg) was analysed (for nigericin: 4107 proteins compared to 1490 proteins; for PMA: 4018 proteins compared to 1535 proteins). An overview of all the proteins associated with NETs released from primary neutrophils and PLB-985 cells after stimulation with PMA or nigericin listed according to their relative abundance can be found in Supplementary Table S1. The abundance of NET proteins grouped based on their function and cellular localisation is displayed in Fig. 1. A large proportion of the identified proteins are classified as nucleic acid binding proteins, metabolic enzymes, cytoskeleton proteins, or proteins involved in immune and stress responses (Fig. 1A). The majority of NET proteins are nuclear or cytoplasmic in origin, though membrane-bound, granule and secreted proteins were also identified (Fig. 1B).

Histones are the most abundant proteins in NETs released from primary neutrophils and PLB-985 cells, following exposure to PMA or nigericin, in accord with previous studies [8–10]. Histone H4 (H4C1) is the most abundant protein in NETs from primary neutrophils after both nigericin and PMA treatment (Table S1). In PLB-985 cells, histone H4 is ranked second after histone H2B type 1-K (H2BC12), following exposure of the cells to each stimulant. Other histones, including H2A (type 1, 1-B/E and 2-B), H2B (type 1-J, 3-B and F–S) and H3 (H3-2 and H3.1) were also highly abundant in the NETs (Table S1). Proteins involved in RNA and mRNA binding, localisation and splicing were also identified in the NETs from each cell type. These proteins include various heterogeneous nuclear ribonucleoproteins (HNRNPU, HNRNPD, HNRNPA1, HNRNPK and HNRNPA1B1), adenylyl cyclase-associated protein 1 (CAP1) and small nuclear ribonucleoprotein-associated proteins B and B' (SNRPB and SNRPN), which vary in abundance depending on cell type and treatment (between abundance rank 20 and 330). In addition, proteins involved in protein binding, folding or synthesis were identified, including inter-alpha-trypsin inhibitor (ITIH2, ITIH3 and ITIH4), the endoplasmic reticulum (ER) chaperone BiP (HSPA5), peptidyl-prolyl *cis*-trans isomerases (PPIA, PPIB and FKBP4), heat shock proteins (HSPA8 and HSP90), ribosomal proteins (RPS16 and RPL12) and elongation factors (EFF1A1 and EEF2; Table S1).

MPO is also a highly abundant protein in the NETs. For both cell types, the abundance of MPO is higher in NETs collected following exposure of the neutrophils to PMA versus nigericin (Table S1). The abundance of MPO is also higher in primary neutrophils relative to PLB-985 cells. In addition to MPO, other proteins with an antimicrobial or immune response function contained within the NETs, include lactotransferrin (LTF) in the PLB-985 cell NETs, annexin A6 (ANXA6), moesin (MSN) and different types of complement proteins (C3 and C7). Cytoskeletal proteins such as actin (ACTB and ACTG1), cofilin-1 (CFL1), plastin-2 (LCP1), profilin-1 (PFN1) and tubulin (TUBA1C, TUBA4A and TUBB) were also abundant NET proteins. Lastly, a number of metabolic or antioxidant enzymes were present in the NETs, including alpha-enolase (ENO1), glyceraldehyde-3-phosphate dehydrogenase (GAPDH), L-lactate dehydrogenase (LDHA and LDHB), transketolase (TKT) and catalase (CAT). Some previously reported NET-associated proteins, such as neutrophil elastase (ELANE), calcium-binding proteins (S100A), myosin-9 (MYH9) and lysozyme C (LYZ) [8–11], were either not detected or only present in low abundance (Table S1).

Comparison of the top 100 most abundant NET proteins released

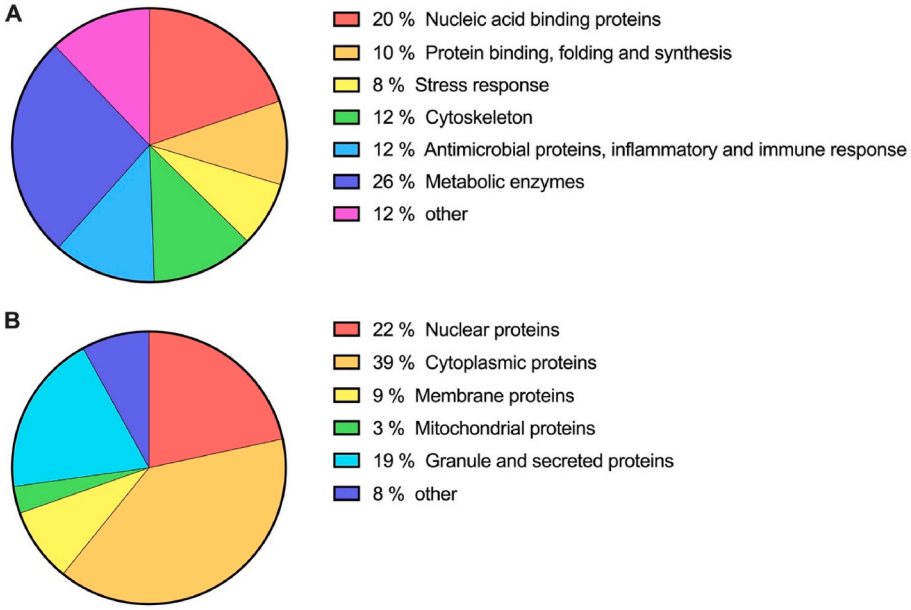

Fig. 1. Pie charts showing the ratio of proteins identified in NETs from primary neutrophils and PLB-985 cells treated with PMA or nigericin grouped based on their function (A) and their localisation (B). Primary neutrophils and differentiated PLB-985 cells were treated with PMA (50 nM) or nigericin (15 μM) for 4 h to release NETs. The supernatant was collected after the addition of DNase I (40 U/μL) to isolate the NETs and the samples were analysed by mass spectrometry. Only the top 50 most abundant proteins in at least one condition (cell type or treatment) and previously identified NET-proteins are grouped based on their function (A) and their localisation (B). The specific proteins and their abundance rank with each cell type and treatment are provided in Supplementary Table S1.

from primary neutrophils after exposure to PMA or nigericin, showed that 71 proteins were common, while 29 proteins were unique to each treatment condition. The most abundant of these 71 common proteins in NETs from primary neutrophils include histone H4, actin, moesin, transketolase, alpha-enolase, catalase, MPO and plastin-2. Beta-enolase, myosin-9 and histone H2B type F–S are uniquely present among the most abundant NET proteins identified from primary neutrophils after PMA treatment, whereas histone H2B type 1-J was exclusively present among the top abundant proteins released from cells exposed to nigericin treatment. Among the top 100 most abundant NET proteins released by primary neutrophils, 24 and 27 proteins were significantly increased after nigericin and PMA treatment, respectively (Fig. 2A). The proteins detected at higher levels after nigericin treatment include catalase (CAT), alpha-actinin-4 (ACTN4), cytoplasmic malate dehydrogenase (MDH1), purine nucleoside phosphorylase (PNP), Cofilin-1 (CFL1) and transaldolase (TALDO1), whereas actin (ACTG1), heat shock protein HSP 90-alpha (HSP90AA1), alpha-enolase (ENO1), MPO, GAPDH, mitochondrial malate dehydrogenase (MDH2), histone H4 (H4C1) and histone H2A type 1-B/E (H2AC4) were detected at higher levels after PMA treatment (Fig. 2A).

Comparison of the top 100 most abundant proteins in NETs released by PLB-985 cells, showed that 81 proteins were common to PMA and nigericin treatment, including transaldolase, alpha-actinin-4, alpha-enolase, histones (H4, H3.1, H2B type 1-K, H3, H2A type 2-B), moesin, profilin-1, transketolase, lactotransferrin, MPO and catalase. With the PLB-985 cells, 19 proteins were found exclusively among the top 100 most abundant NET proteins in NETs from cells exposed to either PMA or nigericin treatment. Several proteins were detected at higher levels in NETs released from PLB-985 cells exposed to PMA treatment, including moesin (MSN), MPO, L-lactate dehydrogenase A chain (LDHA), histones (H4, H2AC21, H1-4), alpha-actinin-4 (ACTN4), actin (ACTB), alpha-enolase (ENO1) and transketolase (TKT; Fig. 2B). In contrast, transitional endoplasmic reticulum ATPase (VCP), tubulin alpha-4A chain (TUBA4A), peptidyl-prolyl *cis*-trans isomerase B (PPIB), transaldolase (TALDO1) and glucose-6-phosphate isomerase (GPI) were detected at higher levels in NETs from PLB-985 cells exposed to nigericin treatment

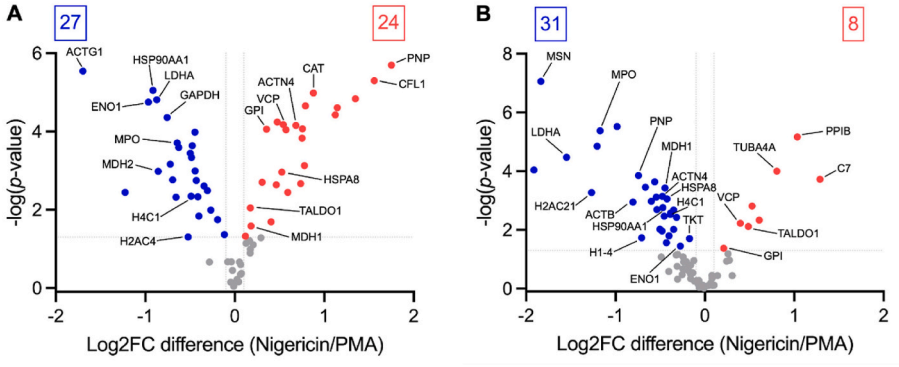

Fig. 2. Volcano plots showing difference in protein abundance in the NETs from primary neutrophils (A) and PLB-985 cells (B) treated with nigericin (15 μM) vs PMA (50 nM). Proteins above a significance threshold of -log(P-value) 1.3 and Log2 fold chance >0.1 are highlighted. Proteins that are more abundant in NETs from cells stimulated by nigericin are shown in red. Proteins that are more abundant in NETs from cells exposed to PMA are shown in blue.

(Fig. 2B).

In both cell types, transitional endoplasmic reticulum ATPase (VCP) and glucose-6-phosphate isomerase (GPI) were detected at higher levels in NETs released following exposure to nigericin (Fig. 2). However, heat shock protein HSP 90-alpha (HSP90AA1), MPO, L-lactate dehydrogenase A chain (LDHA), alpha-enolase (ENO1) and histone H4 (H4C1) were detected at higher levels in NETs released from both cell types following exposure to PMA (Fig. 2). Cytoplasmic malate dehydrogenase (MDH1), heat shock cognate protein 71 kDa (HSPA8) and purine nucleoside phosphorylase (PNP) were detected at higher levels exclusively in NETs from primary neutrophils exposed to nigericin (Fig. 2A). In PLB-985 cells, these proteins are instead detected at higher levels in NETs released following exposure to PMA (Fig. 2B).

The nature of proteins present in NETs released by primary neutrophils was also compared to the proteins present in PLB-985 cell NETs with each stimulus. Considering the 100 most abundant proteins in NETs released following PMA stimulation, 55 proteins were common to primary neutrophils and PLB-985 cells, whereas 45 proteins were exclusively identified in only one cell type (Fig. S2C, Table S1). A similar distribution can be seen in the comparison of primary neutrophils and PLB-985 cells exposed to nigericin treatment (Fig. S2D; 54 proteins in common and 46 cell type specific). However, with both PMA and nigericin treatments, there was a greater number of upregulated proteins in NETs from the primary neutrophils (Fig. S1, proteins coloured in red).

3.2. Proteins in NETs released from primary neutrophils and PLB-985 cells contain multiple types of oxidative PTMs

Oxidative histone modifications induced by HOCl, including Lys nitrile and aminoadipic semialdehyde and Tyr chlorination have previously been observed on exposure of isolated histones to HOCl in vitro [30,31]. Here we have investigated if these oxidative modifications also can be identified in NETs isolated from primary neutrophils and PLB-985 cells. Indeed, evidence is presented for 3-Cl-Tyr formation on several different sites in histone H2A, H3 and H4 (Fig. 3 and Table 1). In addition, chlorination sites are also detected in other NET proteins, including beta-actin-like protein 2, fructose-bisphosphate aldolase C, myosin-10 and quinone oxidoreductase (Table 1 and S3). The majority of these chlorinated peptides were identified in NETs from both cell types following exposure to PMA or nigericin. However, chlorination of Tyr-166 in beta-actin-like protein 2, was only detected in NETs from PLB-985 cells, and chlorination of Tyr-284 in fructose-bisphosphate aldolase C, was found only in NETs from primary neutrophils. There was also evidence for chlorination of Trp-273 on serpin I2, in NETs from both cell types following nigericin treatment (Table 1 and S3). In addition to chlorination, several other types of PTMs were detected on the NET proteins, including oxidation of Met and Lys nitrile or aminoadipic semialdehyde (Table 2 and S3). There was evidence for nitrile formation in histone H3-like centromeric protein A (Lys-123), in neurofilament medium polypeptide (Lys-590, Lys-597), and quinone oxidoreductase (Lys-115) in NETs from both cell types exposed to PMA or nigericin (Table 2 and S3). Aminoadipic semialdehyde was identified in all NETs on Lys-115 in different isoforms of histone H3, and also in other NET proteins, e.g. Lys-203 in transaldolase and Lys-497 in pregnancy zone protein (Table 2 and S3).

NET-associated histones are also known to contain various types of non-oxidative PTMs, including acetylation of Lys and citrullination of Arg [28,29]. Therefore, these modifications were mapped in the NETs from primary neutrophils and PLB-985 cells, released after exposure to PMA or nigericin. The position of the identified acetylation and citrullination sites on histone H2A, H3 and H4 are labelled in Fig. 3. The majority of modified sites from histone H3 (isoforms H3-2, H3C15) and histone H4 were detected in NETs from both cell types and with both stimuli, whereas the modified sites from histone H2A (isoform H2AC20) were only detected in NETs from primary neutrophils (Table S2). Acetylation of Lys-14 in Histone H3.2 and Lys-5 in histone H4 was observed only in NETs from primary neutrophils and PLB-985 cells, respectively (Table S2).

3.3. Chlorination of histone H4 Tyr-88 is more prevalent in NETs from PMA-stimulated cells

Chlorination of Tyr-88 in histone H4 was observed consistently in NETs from primary neutrophils and PLB-985 cells and has previously been detected on exposure of isolated histones to HOCl in vitro [30,31]. Peptides harbouring this chlorination site in histone H4 were detected with and without a missed cleavage at the beginning and end of the peptide, and often with oxidation of the Met residue (Table 1 and S2). Fig. 4 shows the MS/MS fragmentation spectrum for the peptide TVTAMDVVYALKR, with chlorination at Tyr-88 corroborated by a mass shift of +33.96 Da of the y5 to y9 ions of the modified peptide. Chlorination of this peptide is also supported by the increased intensity in [M+2] peaks due to the specific isotope profile of chlorine (abundance of ^{35}Cl is 75 % and for ^{37}Cl is 25 %).

The intensity of the histone H4 modified peptides TVTAM[ox]DVVYALK and TVTAM[ox]DVVY[Cl]ALK were compared under different experimental conditions with each cell type (Fig. 5). The intensity of the histone H4 peptide with Met oxidation TVTAM[ox]DVVYALK from background NET release from non-stimulated PLB-985 cells was significantly increased compared to that on NETs from cells exposed to PMA or nigericin (Fig. 5A, black bars). This may reflect artifactual oxidation, owing to the additional time required to concentrate these samples. This is because the NET release from non-stimulated

Table 1
Chlorination of specific Tyr (Y) and Trp (W) residues observed on NET proteins released by primary neutrophils or PLB-985 cells after stimulation with PMA (50 nM) or nigericin (15 μM) for 4 h. The peptides listed are those that contain a chlorinated (Cl) Tyr (Y) or Tyr (W) residue. Some peptides also have additional modifications such as oxidation (ox) of Met (M) and aminoadipic semialdehyde (sa) or nitrile (ni) formation on Lys (K). The identification of the peptides is based on database searches in Fragpipe followed by manual validation in Skyline as outlined in Section 2.7 of the Materials and Methods. Only the local sequences of the protein are shown. An expanded version of this Table can be found in Supplementary data, Table S3.

Protein	Residue	Local sequence	Treatment	Other modifications
Histone H2A type 1-B/E	Y[Cl]-50	PVY[Cl]LAAV	PMA[a,b], Nigericin[a,b]	
Histone H2A type 1-B/E	Y[Cl]-57	LAAVLEY[Cl]LTA	PMA[b], Nigericin[a,b]	
Histone H3.1t	Y[Cl]-99	EACESY[Cl]LVG	Nigericin[b]	
Histone H3.2	Y[Cl]-99	EASEAY[Cl]LVG … HAK[sa]	PMA[a,b], Nigericin[a,b]	M[ox]-90; K[sa]-115
Histone H4	Y[Cl]-88	DVVY[Cl]ALKR	PMA[a,b], Nigericin[a,b]	M[ox]-84
Beta-actin-like protein 2	Y[Cl]-166	VPIY[Cl]EGYAL	PMA[b], Nigericin[b]	
Fructose-bisphosphate aldolase C	Y[Cl]-223	Y[Cl]TPE	PMA[a], Nigericin[a]	
Myosin-10	Y[Cl]-284	HIFY[Cl]QLL	PMA[a,b], Nigericin[a,b]	
Quinone oxidoreductase	Y[Cl]-102 or Y[Cl]-114	SGGY[Cl]AEYALAADHTVY[Cl]K[ni]	PMA[a,b], Nigericin[a,b]	K[ni]-115
Serpin I2	W[Cl]-273	KW[Cl]LSEM[ox]QEEE	Nigericin[a,b]	M[ox]-277

[a] Indicates identification in NETs from primary neutrophils.
[b] Indicates identification in NETs from PLB-985 cells.

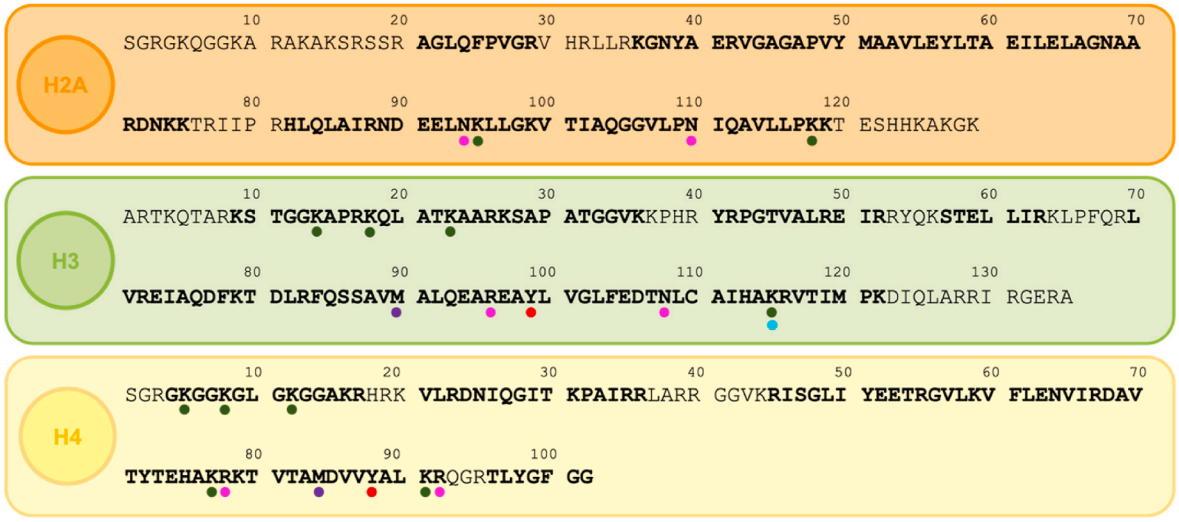

Fig. 3. Post-translational modifications of histone proteins identified in the NETs from primary neutrophils and PLB-985 cells treated with PMA or nigericin. The sequences of H2AC4 and H3-2 are shown as to be representative of the different types of H2A and H3 proteins. The sequence coverage is 67 % for H2A, 74 % for H3 and 83 % for H4 indicated in bold font. Labelling of PTMs: purple for Met oxidation, red for Tyr chlorination, blue for Lys aminoadipic semialdehyde, dark green for Lys acetylation, pink for Arg citrullination.

Table 2
Nitrile and aminoadipidic semialdehyde formation on specific Lys residues observed on NET proteins released by primary neutrophils or PLB-985 cells after stimulation with PMA (50 nM) or nigericin (15 μM) for 4 h. The peptides listed are those that contain aminoadipic semialdehyde (sa) or nitrile (ni) on Lys (K) residues. Some peptides also have additional modifications such as chlorination (Cl) of Tyr (Y) and oxidation (ox) of Met (M). The identification of the peptides is based on database searches in Fragpipe followed by manual validation in Skyline as outlined in Section 2.7 of the Materials and Methods. Only the local sequences of the protein are shown. An expanded version of this Table can be found in Supplementary data, Table S3.

Protein	Residue	Local sequence	Treatment	Other modifications
Histone H3-like centromeric protein A	K[ni]-123	FPK[ni]DVQ	PMA[a,b], Nigericin[a,b]	
Histone H3.1	K[sa]-115	CAIHAK[sa]	PMA[a,b]	M[ox]-90
Histone H3.2	K[sa]-115	Y[Cl]LVGLFEDTNLCAIHAK[sa]	PMA[a,b], Nigericin[a,b]	M[ox]-90; Y[Cl]-99
Alpha-fetoprotein	K[sa]-559	QK[sa]PQITE	PMA[a,b], Nigericin[a,b]	
Cytoplasmic dynein 1 intermediate chain 2	K[sa]-157; K[sa]-168	YTK[sa]ETQTPVMAQPK[sa]	PMA[a,b], Nigericin[a,b]	M[ox]-164
Erlin-2	K[sa]-266	ECYTAMK[sa]	PMA[a,b], Nigericin[a]	M[ox]-265
Fructose-bisphosphate aldolase A	K[sa]-297	LK[sa]PWA	PMA[a,b], Nigericin[a,b]	
Neurofilament medium polypeptide	K[ni]-590; K[ni]-597	EK[ni]SEEVATK[ni]	PMA[a,b], Nigericin[a,b]	
Nucleolin	K[sa]-507	TLQEVFEK[sa]	PMA[a,b]	
Pregnancy zone protein	K[sa]-497	IMAK[sa]	PMA[a,b], Nigericin[a,b]	M[ox]-482; M[ox]-495
Quinone oxidoreductase	K[ni]-115	GGY[Cl]AEYALAADHTVY[Cl]K[ni]	PMA[a,b], Nigericin[a,b]	Y[Cl]-102 or Y[Cl]-114
Transaldolase	K[sa]-203	DKK[sa]	PMA[a,b], Nigericin[a,b]	
Transcription elongation factor A protein 1	K[sa]-18	K[sa]NAAG	PMA[a,b], Nigericin[a,b]	
WD repeat-containing protein 46	K[sa]-226	VTK[sa]K	PMA[a,b]	

[a] Indicates identification in NETs from primary neutrophils.
[b] Indicates identification in NETs from PLB-985 cells.

PLB-985 cells was very low, and consequently, there was a very low protein concentration in the supernatants compared to from the PMA- or nigercin-treated cells. In addition, the level of the TVTAM[ox]DVVYALK peptide will also be decreased if it is further modified by chlorination for example. Indeed, the intensity of the histone H4 chlorinated peptide TVTAM[ox]DVVY[Cl]ALK was significantly increased on NETs collected from PLB-985 cells exposed to PMA, compared to non-stimulated and nigericin-treated cells (Fig. 5B, black bars). With the primary neutrophils, the intensities of the TVTAM[ox]DVVYALK peptide are more similar in the absence and presence of PMA or nigericin compared to the non-stimulated cells (Fig. 5A, grey bars). However, a significant increase in the intensity of the chlorinated TVTAM[ox]DVVY[Cl]ALK peptide is observed on NETs from primary neutrophils exposed to PMA treatment (Fig. 5B, grey bars). Next, the occupancy of chlorination at Tyr-88 was calculated by dividing the sum of the intensity of chlorinated peptides covering this site with the total intensity for all peptides covering this site (see detailed description in Materials and Methods). A significant increase in occupancy was observed in NETs from PMA-treated cells compared to nigericin-treated or non-stimulated cells (Fig. 5C). The overall calculated occupancy of histone H4 Tyr-88 chlorination in the NETs from the PLB-985 cells was significantly decreased relative to primary neutrophils, except for on PMA treatment (Fig. 5C).

3.4. *Chlorination of histone H4 Tyr-88 is detected in nuclear and cytosolic fractions from PLB-985 cells*

To examine whether histone H4 Tyr-88 is chlorinated inside or outside the neutrophil, experiments were performed with PLB-985 cells to analyse histone H4 in different cellular compartments following neutrophil stimulation. Cellular proteins from the cytosolic and nuclear fractions of the PLB-985 cells were isolated and subjected to LC-MS/MS analysis. Initial studies examined whether differentiation (with ATRA/DMSO) of the PLB-985 cells influenced the chlorination of histone H4 Tyr-88. Evidence was obtained for a low extent of Tyr-88 chlorination in histone H4 on lysis of the differentiated cells, which was also seen in the cytoplasmic and nuclear fractions (Fig. 6A). This chlorination could not

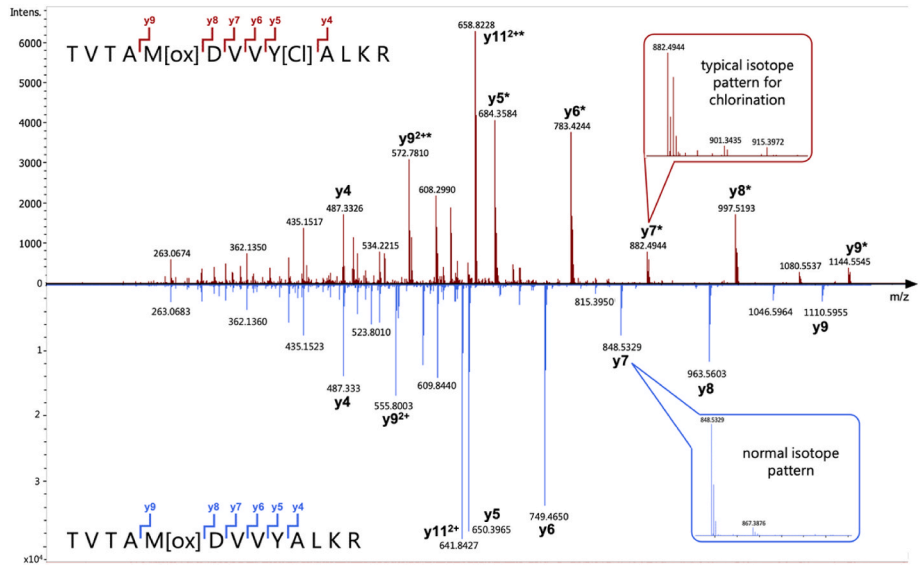

Fig. 4. MS/MS spectra of modified histone H4 peptides. A fragment spectrum of the TVTAMDVVYALKR peptide modified by oxidation of Met-84 and chlorination of Tyr-88 (top, in red) is compared with a spectrum of the corresponding peptide modified by oxidation of Met-84 but lacking chlorination of Tyr-88 (bottom, in blue). The y-ions 5–9 in the top spectrum show the typical isotope pattern for chlorination (illustrated for y7) and the *m/z* values for the peaks for y5-y9 indicate the mass shift of +33.96 Da (highlighted as *) compared to the corresponding fragment ions in the bottom spectrum.

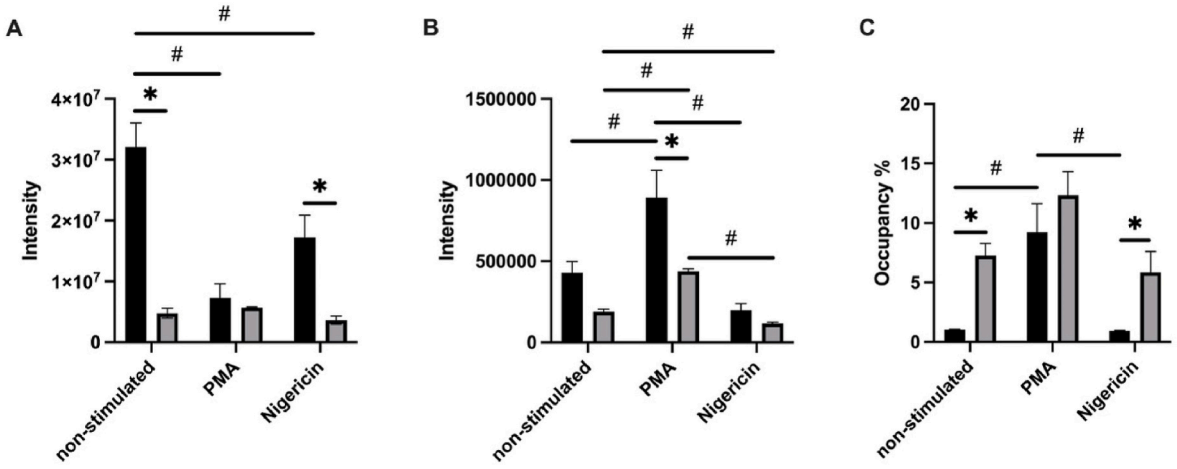

Fig. 5. Modification of the histone H4 peptide TVTAMDVVYALK from NETs collected from primary neutrophils and PLB-985 cells stimulated with PMA or nigericin. Intensity of the TVTAM[ox]DVVYALK (A) and TVTAM[ox]DVVY[Cl]ALK (B) peptides, and occupancy of the chlorination site Tyr-88 of histone H4 peptide TVTAMDVVYALK (C), are shown, calculated as outlined in Section 2.7 of the Materials and Methods. Data represent the mean ± SEM of at least 3 independent experiments. Results from the PLB-985 cells and primary neutrophils are displayed as black bars and grey bars, respectively. * shows a significant ($p < 0.05$) difference by two-way ANOVA with Šídák's multiple comparisons post-hoc test for comparison between different cell types and # shows a significant ($p < 0.05$) difference by one-way ANOVA with Tukey's multiple comparisons post-hoc test for comparison between treatments (stimuli).

be detected in any of the cellular compartments or lysates of the non-differentiated PLB-985 cells (data not shown).

Exposure of the PLB-985 cells to PMA for 4 h, resulted in NET release, with chlorination of Tyr-88 in histone H4 seen in the cytoplasmic and nuclear cellular fractions, as well as the NETs (Fig. 6B). There was no significant difference in occupancy between NETs and each cellular fraction, suggesting a similar extent of histone H4 chlorination in each case (Fig. 6B). This suggests that chlorination of histone H4 may be occurring concurrently with NET release into the extracellular environment. Chlorination of histone H4 Tyr-88 was also observed in the NETs and both cellular fractions of PLB-985 cells exposed to nigericin (Fig. 6C). However, a significant increase in occupancy was observed in the NETs relative to the cytoplasmic and nuclear extracts of the PLB-985 cells in this case (Fig. 6C).

3.5. Chlorination of histone H4 Tyr-88 is diminished in cells exposed to the MPO inhibitor AZD5904

Experiments were also performed to examine whether the chlorination of histone H4 at Tyr-88 was dependent on the activity of MPO using the inhibitor AZD5904. It has been shown previously that stimulation of PLB-985 cells with PMA results in the formation of HOCl, which is not seen on stimulation of the cells with nigericin [38]. Therefore, to optimise the concentration of MPO inhibitor, experiments were performed using R19-S to measure HOCl production in PLB-985 cells exposed to PMA, in the absence and presence of varying amounts of AZD5904. A significant decrease in HOCl formation by the PLB-985 cells was observed with 0.5–1 μM of AZD5904, with complete inhibition seen with 10 μM (Fig. S3). Thus, AZD5904 was added to a final concentration of 10 μM in the subsequent MS experiments.

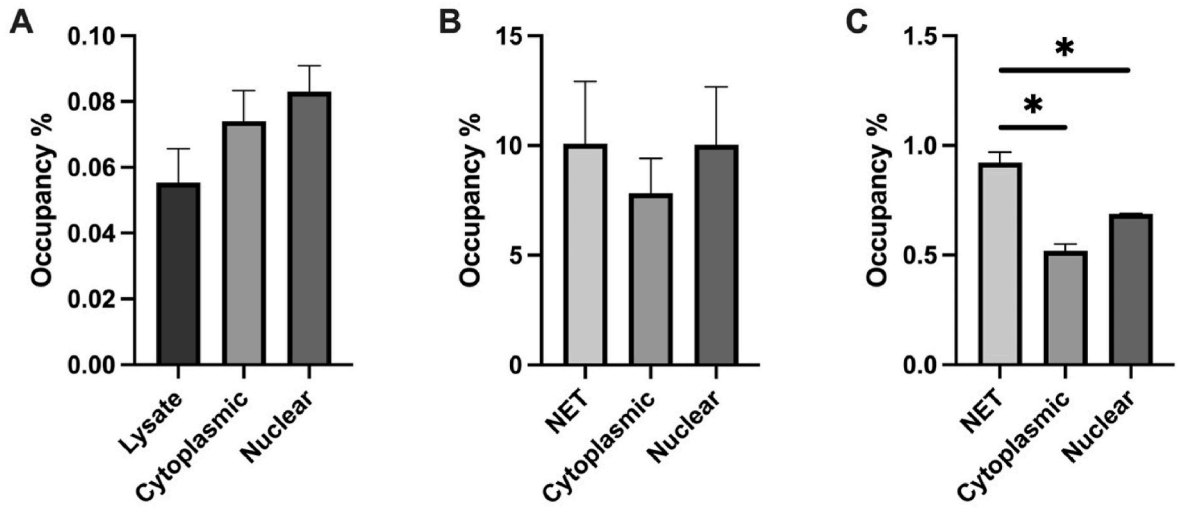

Fig. 6. Chlorination of Tyr-88 of histone H4 is seen in cellular fractions and NETs from differentiated PLB-985 cells. Graphs show occupancy of histone H4 Tyr-88 chlorination in differentiated PLB-985 cells A) without further stimulation or incubation (whole cell lysate, cytoplasmic and nuclear fractions), B) on exposure to PMA (50 μM or C) on exposure to nigericin (15 μM) for 4 h (NET, cytoplasmic and nuclear fractions). The occupancy was calculated as described in Section 2.7 of the Materials and Methods. Data represent mean ± SEM from at least 3 independent experiments and are expressed as percent occupancy. * shows a significant ($p < 0.05$) difference by one-way ANOVA with Tukey's multiple comparisons post-hoc test.

The MS experiments to examine histone H4 chlorination on NETs from PLB-985 cells incubated with AZD5904 to inhibit MPO were performed with nigericin-treated PLB-985 cells, as inhibition of MPO is reported to significantly decrease NET release in PMA-stimulated cells [43]. Treatment of the PLB-985 cells with AZD5904 prior to exposure to nigericin resulted in a significant decrease in the extent of chlorination of Tyr-88 on histone H4 in the NETs based on occupancy calculations (Fig. 7A). It appears that inhibition of MPO also decreases the abundance of histone H4 present within the NETs released following nigericin treatment, based on the general intensity of histone H4 at the protein level, however, the change was not statistically significant (Fig. 7B). A significant decrease in the chlorination occupancy at Tyr-88 in histone H4 was observed on the NETs released from non-stimulated cells (data not shown). Here, there was also no difference in the abundance of histone H4 at the protein level in the presence or absence of AZD5904 in the NETs (data not shown). Together, these data are consistent with a role for MPO in the chlorination of histone H4 seen in NETs from PLB-985 cells.

3.6. Histone H4 Tyr-88 chlorination detected in patient samples

To determine whether chlorination of Tyr-88 on histone H4 could be detected more widely, particularly in NETs from neutrophils isolated from patients with different inflammatory diseases, published, publicly available, MS datasets were examined. Database searches confirmed the chlorination of Tyr-88 from histone H4 in NETs derived from neutrophils isolated from patients with systemic lupus erythematosus (SLE) and rheumatoid arthritis (RA) stimulated with PMA *ex vivo*.

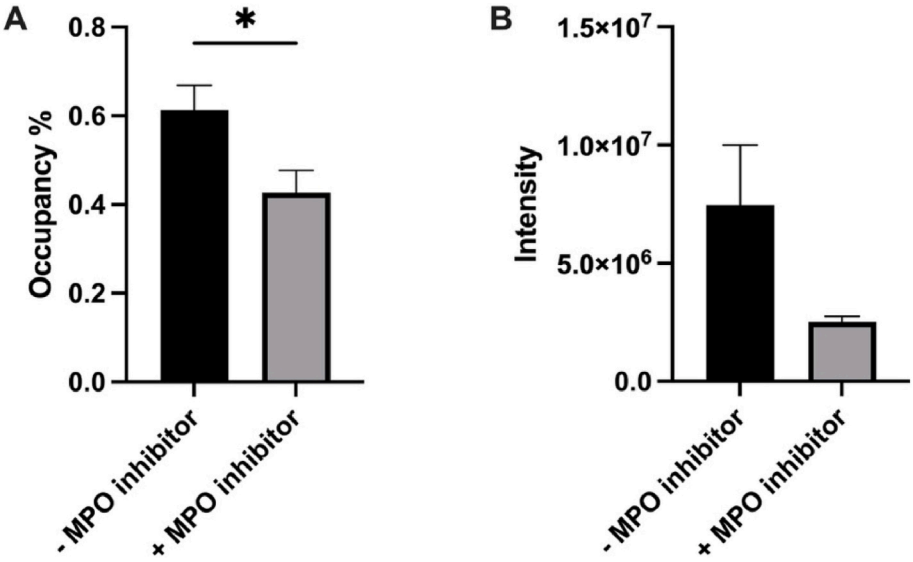

Fig. 7. Inhibition of MPO decreases the chlorination of histone H4 Tyr-88 in NETs from PLB-985 cells. Panel (A) shows the occupancy of the chlorination site (Tyr-88) of histone H4 in NETs collected from PLB-985 cells pre-treated with the MPO inhibitor AZD5904 for 15 min before stimulation with nigericin (15 μM) for 4 h and collection of NETs, calculated as outlined in Section 2.7 of the Materials and Methods. Panel (B) shows the intensity of histone H4 based on analysis of the DIA protein intensity. Data represent mean ± SEM from at least 3 independent experiments and are expressed as A) percent occupancy and B) DIA protein intensity. * shows a significant ($p < 0.05$) difference by unpaired *t*-test.

Interestingly, there was a trend of an increase in occupancy of chlorination at this Tyr residue in NETs from SLE and RA patients following PMA stimulation compared to corresponding samples from healthy donors (Fig. 8). There was also evidence for chlorination of Tyr-88 on histone H4 on NETs released from neutrophils stimulated with the calcium ionophore A23187 (Fig. 8). In general, the chlorination occupancy is lower in the published dataset compared to our present study, including in experiments with PMA to stimulate NET release. We also found evidence for the chlorination of Tyr-88 of histone H4 in intact neutrophils isolated from blood samples collected from patients with COVID-19 (Figure S4 [44]). This provides additional evidence that the chlorination of histone H4 can occur prior to NET release.

3.7. Solvent accessibility of Tyr-88 of histone H4

Histone H4 is one of the most abundant proteins within the NETs from each type of neutrophil and following exposure to PMA or nigericin (Table S1). Tyr-88 is known to be a favoured site for chlorination by HOCl in experiments with isolated histone H4, on account of the YXXK/KXXY sequence motif [30,31]. To examine whether the susceptibility of Tyr-88 of histone H4 to modification by HOCl on NETs may also be favoured owing to its position within the nucleosome structure, we performed solvent accessible surface area (SASA) calculations using an online tool for determination of accessible surface area and accessibility calculation for proteins (http://cib.cf.ocha.ac.jp/bitool/ASA/). Scores between 0 and 1 indicate a relative accessibility (0–100 %), with values closer to 1 being more solvent accessible. The PDB entry 3AFA was used for these calculations, which represents the structure of the 2 histone H4 chains (B-chain and F-chain) within the nucleosome core histone octamer surrounded by DNA [45]. Tyr-88 was shown to be the most solvent accessible Tyr residue on both the B-chain and F-chain of histone H4 within the nucleosome octamer, with a relative accessibility score of 0.15, compared to Tyr-51, 72 and 98, which had scores of 0.07, 0.02 and 0.005, respectively (Fig. 9, Supplementary Video S1). These values were supported by corresponding b-factor and occupancy parameters that also had a higher value for Tyr-88, indicating greater flexibility and surface exposure, in this region of the histone H4 chain (data not shown). These results suggest that Tyr-88 of the core histone H4 is more exposed to the surface of the nucleosome compared to the other Tyr residues (Fig. 9, Supplementary Video S1). This may facilitate chlorination by HOCl prior to, or during, the pathway of NET release.

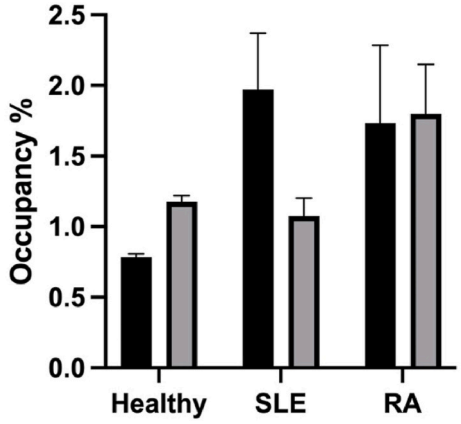

Fig. 8. Chlorination of Tyr-88 of histone H4 is seen in NETs collected from neutrophils from patients with systemic lupus erythematosus (SLE), rheumatoid arthritis (RA) or healthy patients. Raw MS DDA data was downloaded from proteomeexchange.org (identifier PXD011796 [29]) and subjected to database searches, with the occupancy of Tyr-88 chlorination calculated as outlined in Section 2.7 of the Materials and Methods. As described in Chapman et al. the neutrophils were treated *ex vivo* with PMA (50 nM) or A23187 (3.8 μM) for 4 h to produce NETs, which were digested with trypsin and the peptides analysed by LC-MS/MS using a QExactive HF quadrupole-orbitrap mass spectrometer [29]. The results of the PMA-treated samples are displayed as black bars (healthy: n = 3; SLE: n = 6; RA: n = 5) and the results of the A23187-treated samples are displayed as grey bars (healthy: n = 3; SLE: n = 6; RA: n = 4).

4. Discussion

NETs are strongly implicated in disease, particularly in acute and chronic inflammatory environments, but there is no information as to whether they are subjected to oxidative modifications. This is significant in light of recent data showing that modification of histones alters their reactivity in the extracellular environment with different cell types in a pro-inflammatory manner [34,36,46]. Evidence was obtained for oxidative modification of Lys, Tyr and Met residues on different histones in NETs released from primary neutrophils and PLB-985 cells, particularly on stimulation of the cells with PMA. There was strong evidence for the chlorination of Tyr-88 on histone H4 on the NETs from both cell neutrophil cell types. Importantly, this HOCl-induced histone modification was detected on NETs released from neutrophils isolated from patients with autoimmune diseases, including SLE and RA. There was also evidence for oxidative modifications on other, less abundant NET proteins, including quinone oxidoreductase, myosin-10 and transaldolase.

Proteomics analysis of the NETs from the primary neutrophils, revealed a high abundance of nucleic acid binding proteins, particularly histones, cytoskeletal proteins, metabolic enzymes, together with proteins that are involved in immune and stress responses, in accord with previous studies [8–10]. Interestingly, there was also evidence for the presence of mitochondrial proteins. Mitochondria can contribute to NETosis by mediating ROS production, and/or by releasing mitochondrial DNA (mtDNA) extracellularly [47]. The mechanisms responsible for the release of mtDNA have not been fully characterised, but the localisation of mitochondria to the plasma membrane prior to mtDNA release or mitochondrial rupture in the cytosol could both potentially contribute to the presence of mitochondrial proteins within the NETs.

There was a similar distribution of proteins identified within the NETs released from PLB-985 cells, with histones and MPO found to be amongst the most abundant proteins, particularly on stimulation of the cells with PMA. However, there was an absence of some proteins reported previously to be abundant in NETs, including neutrophil elastase, which could only be detected in NETs from primary neutrophils with very low abundance and appeared to be absent in NETs from PLB-985 cells. This result is surprising, given that NETs display proteolytic activity characteristic of neutrophil elastase [9], and are involved in the mechanism of NETosis [48]. This may be related to the methodology used to isolate the NETs and prepare the proteins for digestion and proteomic analysis. Previous studies show that the tight binding of neutrophil elastase to DNA means that its detection in NETs is influenced by the nuclease digestion step used during sample preparation [8,9]. Here, the NETs were exposed to DNase I for 10 min, compared to longer incubation times >30 min in previous studies [8–10], which could contribute to low abundance of neutrophil elastase observed here.

The majority (~75 %) of the abundant NET proteins are common to NETs released from neutrophils stimulated by PMA and nigericin, though these compounds induce NETosis primarily by NOX dependent and independent mechanisms, respectively [7]. Histone H4 is the most abundant protein in NETs from primary neutrophils and ranks second behind histone H2B, in NETs from PLB-985 cells, with both stimuli. MPO is more abundant in the NETs released following stimulation of the neutrophils by PMA compared to nigericin, which may reflect the requirement of MPO and involvement of HOCl in driving NETosis in this case [16,17]. Interestingly, α-enolase is more abundant in NETs from cells stimulated with PMA compared to nigericin, which contrasts with a proteomic analysis comparing NETs from neutrophils stimulated with the Ca^{2+} ionophore A23187, which also triggers NETosis by a pathway independently of NOX [29]. Similarly, there was no evidence for the

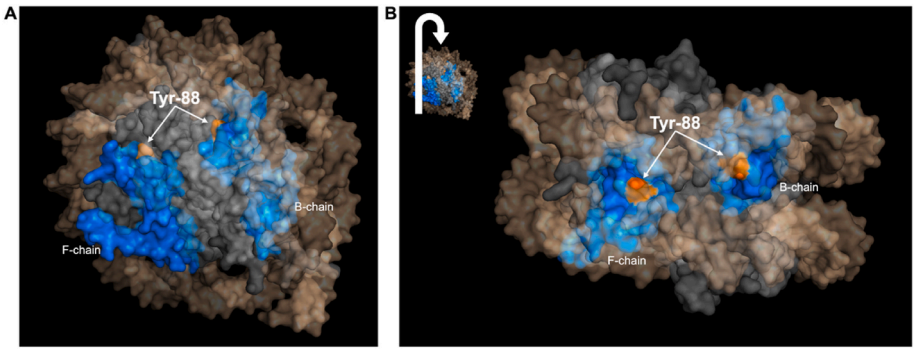

Fig. 9. Image showing the surface accessibility of Tyr-88 of histone H4 in the nucleosome complex. The image shows the localisation of Tyr-88, coloured in orange within the F-chain and B-chain of histone H4 coloured in blue, in the nucleosome complex structure, based on PDB entry 3AFA [44]. The other core histones (H2A, H2B, and H3) are coloured in grey and the DNA is coloured in light brown. See Supplementary Video S1 for a rotating image highlighting the position of Tyr-88 in histone H4.

enrichment of histone H1, matrix metalloproteinase 8 (MMP8), cathelicidin antimicrobial peptide (CAMP/LL37), cysteine-rich secretory protein 3 (CRISP3), or lipocalin on NETs from neutrophils exposed to nigericin, in contrast to studies with A23187 [29]. The differences between the protein composition of NETs from each ionophore (nigericin and A23187) may reflect the ability of nigericin to stimulate the inflammasome, in addition to its action as a K^+ ionophore [21]. This is because inflammasome activation will promote the release of cytokines, including IL-1β, IL-18, which can also stimulate NET release, but by a NOX-dependent pathway [49]. Further studies are needed with a wider range of inducers of NOX dependent and independent pathways of NETosis, as both are pathologically relevant. In addition, recent studies show that nigericin alters Golgi organisation and function, which enhances the Golgi recruitment of NLPR3 during activation of the inflammasome [50]. Whether nigericin-induced reorganization of the Golgi apparatus plays a role in NETosis is not clear, though the remodeling of other cellular organelles, particularly the ER, is important during lytic release of NETs [47].

Transaldolase is the only protein that is upregulated in both cell types by nigericin treatment, suggesting that it may be involved in NET release in this case. Transaldolase is a non-oxidative enzyme in the pentose phosphate pathway (PPP) that converts ribulose-5-phosphate to nucleic acids or glycolytic precursors and ultimately lactate or pyruvate. The production of NADPH by the PPP is involved in NET release, but the formation of glycolytic precursors by the non-oxidative enzymes, including transaldolase, is also important [51]. The oxidative burst and NET release are reduced in neutrophils deficient in transaldolase [51]. However, the dependence of the PPP on NET release is usually associated with NOX-dependent pathways activated by PMA rather than Ca^{2+}influx driven by ionophores [51,52]. Thus, the reason for the enrichment of transaldolase within the NETs from nigericin-treated neutrophils is unexpected. It is possible that downstream products of glycolysis and the PPP, particularly lactate, could also be involved in NET release in neutrophils exposed to nigericin, particularly as lactate dehydrogenase is also abundant within the NETs. The role of lactate in NET release is controversial but addition of lactate can stimulate NETosis [52,53]. However, further studies are required to fully elucidate the differences in neutrophil metabolism during NET release following exposure to oxidative and non-oxidative stimuli, such as PMA and nigericin.

There is a greater than 50 % similarity in the protein composition of NETs from primary neutrophils and PLB-985 cells, particularly proteins reported previously to be highly abundant in NETs [8–10]. This highlights further that PLB-985 cells are a useful model of NET release, in accord with previous studies [38,54,55]. However, the number of proteins identified in the NETs from the primary cells was greater compared to that from the PLB-985 cells. The extent of NET release observed from primary neutrophils is greater than that of the differentiated PLB-985 cells under comparable conditions, as assessed by quantification of extracellular DNA release using fluorescent DNA-binding dyes [38]. With PMA, this may reflect the stronger oxidative burst and production of HOCl, which is typically in the μM rather than nM range for primary neutrophils and PLB-985 cells respectively [15,38,56]. Together, this may contribute to a higher number of identified proteins present in the NETs from primary neutrophils, which require less concentration for proteomic analysis compared to the PLB-985 cells.

Importantly, our proteomic analysis revealed oxidative modification of histones and other proteins present within NETs released from neutrophils and PLB-985 cells. The detection of chlorinated Tyr residues on histone H2A (Tyr-50) and (Tyr-57), histone H3.1 and H3.2 (Tyr-99), and histone H4 (Tyr-88) is consistent with the production of HOCl by MPO during neutrophil activation and NETosis. This is supported by evidence for the formation of aminoadipic semialdehyde on Lys-115 in Histones H3.1 and H3.2, which is another common modification resulting from the exposure of proteins to HOCl and *N*-chloramine decomposition [32,57]. These histone modifications have been previously identified on isolated histones exposed to HOCl [30,31]. There was also evidence for Met oxidation, which is expected, as Met residues are a favoured site of reaction for HOCl [32,58]. It is possible that Met sulfone (dioxidation) is formed in addition to Met sulfoxide (monooxidation), which was not examined here, owing to software limitations. However, Met dioxidation was only observed in previous studies with isolated histones at relatively high molar excesses of HOCl [30], which may be difficult to achieve on stimulation of neutrophils.

It is possible that the reaction of HOCl with histones could be favoured in NETs owing to the close localisation of MPO and histones on the DNA backbone. However, besides histones, oxidative PTMs were identified on other NET associated proteins including quinone oxidoreductase, where there was evidence for chlorination of Tyr-102, Tyr-114 and nitrile formation on Lys-115. The formation of Lys nitriles further supports a role for HOCl modification, with this product also formed as a result of *N*-chloramine decomposition [32,57]. Interestingly, this protein has not previously been reported to be present in NETs, but it is highly abundant in macrophage extracellular traps [12]. Quinone oxidoreductase is a stress response protein that enables quinone reduction using NADPH or NADH and as such can modulate NAD(P)H:NAD(P)$^+$ levels and neutralise superoxide [59]. However, whether quinone oxidoreductase plays a role in extracellular trap release, and the significance (if any) of its oxidative modification are not known.

The chlorination of Tyr-88 in histone H4 was prevalent on the NETs released from neutrophils and PLB-985 cells, particularly in cells exposed to PMA, which stimulates HOCl production. The calculated occupancy of histone H4 Tyr-88 chlorination in NETs from PLB-985 cells was lower than NETs from primary neutrophils, which likely reflects the

higher concentration of HOCl produced on activation of the primary neutrophils compared to the PLB-985 cells, as outlined above [15,38,56]. This Tyr residue is also a favoured chlorination site in experiments with isolated histones and HOCl [30,31]. This residue is part of a YXXK/KXXY sequence motif, which may be a favoured chlorination site, as the proximal Lys residue acts as the primary target of HOCl, and readily transfers chlorine to Tyr [31,60]. That this Tyr (and Lys) residue lies in a surface exposed position within the nucleosome structure may also be important, particularly as there is evidence for the chlorination of Tyr-88 of histone H4 in the nucleus of the PLB-985 cells and neutrophils isolated from COVID-19 patients [44], as well as in the released NET.

There was no significant difference between histone H4 Tyr-88 chlorination occupancy in NETs compared to nuclear and cytosolic extracts from PLB-985 cells exposed to PMA, suggesting that this residue may be chlorinated inside the cell prior to NET release. This is supported by studies showing that MPO enters the nucleus by a process referred to as targeted nuclear degranulation, which promotes histone depolymerisation prior to NET release [61]. In addition, results from real-time imaging studies show MPO activity within the neutrophils rather than on the NETs themselves during NETosis following stimulation of neutrophils with PMA [62]. With nigericin treatment, the chlorination of Tyr-88 is 10-fold lower than that seen in experiments with PMA, consistent with the proposed NOX independent pathway of NET release [7]. That chlorination is observed, may reflect the basal activation of the cells resulting from their isolation from buffy coat preparations or differentiation with ATRA/DMSO. This is supported by the observation that there is no significant difference between the extent of chlorination of histone H4 Tyr-88 in the NETs from non-stimulated and nigericin-treated cells. However, it is also possible that the ability of nigericin to stimulate the inflammasome [21] and promote release of cytokines could induce some NET release by a NOX dependent pathway, as described above.

Further support for the role of MPO in driving the chlorination of histone H4 (and other NET proteins) was obtained in experiments using the inhibitor AZD5904, at a concentration that prevents PMA-induction of HOCl formation. These experiments were not performed with PMA-treated PLB-985 cells as inhibition of MPO and/or HOCl scavenging significantly decreases NETosis [38]. Based on occupancy calculations, the chlorination of histone H4 in NETs from nigericin-treated PLB-985 cells was significantly decreased on pre-treating the cells with AZD5904 to inhibit MPO. However, under these conditions, inhibition of MPO may also decrease the release of NETs, as seen by a decrease in the intensity of the parent histone H4 protein. This was unexpected, as inhibition of MPO using the nitroxide TEMPO, had no effect on NET release by neutrophils or PLB-985 cells exposed to nigericin [38]. A significant decrease in histone H4 chlorination was also observed on inhibition of MPO in the non-stimulated PLB-985 cells, but in this case, there was no change in the extent of release of the histone H4 protein.

Evidence was obtained for citrullination, acetylation, and a range of oxidative modifications on different types of histones present in NETs. Citrullination of histones is used extensively as a marker of NET release [2,7], though there are some circumstances where NET release can occur independently of citrullination [13]. Evidence was obtained for the citrullination of histones H2A, H3 and H4, but not histone H1. The lack of citrullination of histone H1 contrasts to previous studies [29], but may result from the low abundance of this histone in our samples. Moreover, the citrullination site detected on histone H3 (Arg-96) differs from that reported previously in NETs from neutrophils collected from patients with SLE and RA (Arg-26) [29]. It is important to note that peptides citrullinated at the C-terminal Arg residues (trypsin cleavage site) have been excluded, as the modification should result in a missed cleavage [63]. Interestingly, citrullination of histone H4 was not reported previously by Chapman et al. [29]. However, the data in relation to the acetylation of Lys residues, another common histone PTM associated with NETs [28] on histone H4 histone are quite comparable with evidence for modification of Lys-5, Lys-8, and Lys-12 in each case [29].

The functional importance of histone PTMs in the regulation of key cellular events relating to nuclear DNA binding, including transcription, replication, recombination and DNA repair is well established [24] and PTMs on nuclear histones have also been linked to diseases, including cancer [64]. There is also growing interest in understanding how the modification of histones by metabolically produced ROS influences the structure of chromatin and gene expression [65]. The effects of the HOCl-induced histone modifications observed in nucleus of the stimulated neutrophils prior to or during NETosis and on the NETs themselves, need further examination. The oxidative modifications seen here on histones in NETs will be most relevant in the extracellular environment, where histones drive cytotoxic, pro-inflammatory and pro-coagulant reactions, culminating in organ failure and death in many human diseases, including sepsis, COVID-19, atherosclerosis, RA, and SLE [66–68]. Currently, there is only a limited understanding of how histone PTMs influence these reactions. However, citrullination and HOCl-induced modifications of histones have been shown to alter their reactivity in the extracellular environment, to potentiate their pro-inflammatory properties [34,36,46], which is likely to have relevance in vivo.

This, together with evidence presented here for the chlorination of Tyr-88 on histone H4 in NETs from neutrophils isolated from patients with RA and SLE, where the extent of chlorination was greater than that seen in the NETs from neutrophils from healthy controls (data from Ref. [29]), lends further support that HOCl-induced histone modification has biological relevance. Whether chlorination of histone H4 Tyr-88 also has value as a potential biomarker for acute and chronic inflammation needs further investigation, but it is notable that we observed this modification in a published MS dataset from neutrophils isolated from blood samples from COVID-19 patients, with no enrichment or purification of the histones (data from Ref. [44]). Moreover, histone H4 is a key player in driving inflammation and lytic cell death in atherosclerosis [69].

In conclusion, we provide the first evidence that NETs contain proteins modified by the MPO-derived oxidant HOCl. The abundant histones, particularly histone H4, are particular targets, shown by the chlorination of Tyr-88, with Tyr chlorination and other modifications, including Lys aminoadipic semialdehyde and nitrile from *N*-chloramine decomposition also seen on histones H2A and H3. The detection of chlorinated histone H4 within the nuclear and cytoplasmic extracts of the neutrophils suggests that modification may occur prior to NETosis. However, further experiments are required to confirm this, and given close association of MPO and histones, it is likely that further modification can occur on the NETs in the presence of H_2O_2 [33]. While there are some differences in the cellular mechanisms involved in PMA and nigericin induced NETosis, it is notable that both stimulants trigger the release of NETs by a suicidal pathway, which culminates in neutrophil cell death [7]. It will be important in future studies to perform additional experiments with NET collected under conditions that favour vital NETosis, where the viability of the neutrophil is maintained, to see how this affects the protein composition and nature of post-translational modifications. Taken together, the detection of novel oxidative protein modifications, particularly on NET histones, provides new insight into pathways by which these structures could contribute to pathological conditions, particularly in inflammatory conditions.

Funding statement

This work was supported by grants from the Novo Nordisk Foundation (Biomedical Project Grant NNF22OCO0080414 to CH), the Royal Society of Chemistry (Development Grant, R21-4699728863 to CH), and the Carlsberg Foundation (CF19-0451 to PH).

CRediT authorship contribution statement

Helen Hemmling: Writing – review & editing, Writing – original

draft, Methodology, Investigation, Formal analysis, Data curation. **Line A.E. Hallberg:** Supervision, Methodology, Investigation, Data curation. **Per Hägglund:** Writing – review & editing, Supervision, Methodology, Funding acquisition, Formal analysis. **Clare L. Hawkins:** Writing – review & editing, Writing – original draft, Supervision, Resources, Project administration, Funding acquisition, Formal analysis, Conceptualization.

Declaration of competing interest

The authors declare that they have no known competing financial interests or personal relationships that could have appeared to influence the work reported in this paper.

Acknowledgments

The authors would like to thank Professor Michael Davies for helpful discussions and providing access to the Bruker TIMS TOF PRO mass spectrometer used in this study (funded by the Novo Nordisk Foundation, grant number NNF205A0064214).

Appendix A. Supplementary data

Supplementary data to this article can be found online at https://doi.org/10.1016/j.redox.2025.103696.

Data availability

The MS proteomics data have been deposited to the ProteomeXchange Consortium via the PRIDE partner repository [70] with the dataset identifier PXD060348.

References

[1] N. Borregaard, Neutrophils, from marrow to microbes, Immunity (Camb., Mass.) 33 (5) (2010) 657–670, https://doi.org/10.1016/j.immuni.2010.11.011.
[2] V. Papayannopoulos, Neutrophil extracellular traps in immunity and disease, Nat. Rev. Immunol. 18 (2) (2018) 134–147, https://doi.org/10.1038/nri.2017.105.
[3] Y. Doring, P. Libby, O. Soehnlein, Neutrophil extracellular traps participate in cardiovascular diseases: recent experimental and clinical insights, Circ. Res. 126 (9) (2020) 1228–1241, https://doi.org/10.1161/CIRCRESAHA.120.315931.
[4] S.R. Clark, A.C. Ma, S.A. Tavener, B. McDonald, Z. Goodarzi, M.M. Kelly, K. D. Patel, S. Chakrabarti, E. McAvoy, G.D. Sinclair, E.M. Keys, E. Allen-Vercoe, R. Devinney, C.J. Doig, F.H. Green, P. Kubes, Platelet TLR4 activates neutrophil extracellular traps to ensnare bacteria in septic blood, Nat. Med. 13 (4) (2007) 463–469, https://doi.org/10.1038/nm1565.
[5] Y. Zuo, M. Zuo, S. Yalavarthi, K. Gockman, J.A. Madison, H. Shi, W. Woodard, S. P. Lezak, N.L. Lugogo, J.S. Knight, Y. Kanthi, Neutrophil extracellular traps and thrombosis in COVID-19, J. Thromb. Thrombolysis 51 (2) (2021) 446–453, https://doi.org/10.1007/s11239-020-02324-z.
[6] O. Goldmann, E. Medina, The expanding world of extracellular traps: not only neutrophils but much more, Front. Immunol. 3 (420) (2012) 1–10, https://doi.org/10.3389/fimmu.2012.00420.
[7] E.F. Kenny, A. Herzig, R. Kruger, A. Muth, S. Mondal, P.R. Thompson, V. Brinkmann, H.V. Bernuth, A. Zychlinsky, Diverse stimuli engage different neutrophil extracellular trap pathways, eLife 6 (2017) 24437, https://doi.org/10.7554/eLife.24437.
[8] C.F. Urban, D. Ermert, M. Schmid, U. Abu-Abed, C. Goosmann, W. Nacken, V. Brinkmann, P.R. Jungblut, A. Zychlinsky, Neutrophil extracellular traps contain calprotectin, a cytosolic protein complex involved in host defense against Candida albicans, PLoS Pathog. 5 (10) (2009) e1000639, https://doi.org/10.1371/journal.ppat.1000639.
[9] A.J. O'Donoghue, Y. Jin, G.M. Knudsen, N.C. Perera, D.E. Jenne, J.E. Murphy, C. S. Craik, T.W. Hermiston, Global substrate profiling of proteases in human neutrophil extracellular traps reveals consensus motif predominantly contributed by elastase, PLoS One 8 (9) (2013) e75141, https://doi.org/10.1371/journal.pone.0075141.
[10] C.H. Lim, S.S. Adav, S.K. Sze, Y.K. Choong, R. Saravanan, A. Schmidtchen, Thrombin and plasmin alter the proteome of neutrophil extracellular traps, Front. Immunol. 9 (2018) 1554, https://doi.org/10.3389/fimmu.2018.01554.
[11] M. Bruschi, A. Petretto, L. Santucci, A. Vaglio, F. Pratesi, P. Migliorini, R. Bertelli, C. Lavarello, M. Bartolucci, G. Candiano, M. Prunotto, G.M. Ghiggeri, Neutrophil extracellular traps protein composition is specific for patients with lupus nephritis and includes methyl-oxidized alphaenolase (methionine sulfoxide 93), Sci. Rep. 9 (1) (2019) 7934, https://doi.org/10.1038/s41598-019-44379-w.
[12] M. Jensen, N.W. Thorsen, L.A.E. Hallberg, P. Hagglund, C.L. Hawkins, New insight into the composition of extracellular traps released by macrophages exposed to different types of inducers, Free Radic. Biol. Med. 202 (2023) 97–109, https://doi.org/10.1016/j.freeradbiomed.2023.03.025.
[13] S. Boeltz, P. Amini, H.J. Anders, F. Andrade, R. Bilyy, S. Chatfield, I. Cichon, D. M. Clancy, J. Desai, T. Dumych, N. Dwivedi, R.A. Gordon, J. Hahn, A. Hidalgo, M. H. Hoffmann, M.J. Kaplan, J.S. Knight, E. Kolaczkowska, P. Kubes, M. Leppkes, A. A. Manfredi, S.J. Martin, C. Maueroder, N. Maugeri, I. Mitroulis, L.E. Munoz, D. Nakazawa, I. Neeli, V. Nizet, E. Pieterse, M.Z. Radic, C. Reinwald, K. Ritis, P. Rovere-Querini, M. Santocki, C. Schauer, G. Schett, M.J. Shlomchik, H.U. Simon, P. Skendros, D. Stojkov, P. Vandenabeele, T.V. Berghe, J. van der Vlag, L. Vitkov, M. von Kockritz-Blickwede, S. Yousefi, A. Zarbock, M. Herrmann, To NET or not to NET:current opinions and state of the science regarding the formation of neutrophil extracellular traps, Cell Death Differ. 26 (3) (2019) 395–408, https://doi.org/10.1038/s41418-018-0261-x.
[14] P. Patriarca, R. Cramer, M. Marussi, F. Rossi, D. Romeo, Mode of activation of granule-bound NADPH oxidase in leucocytes during phagocytosis, Biochim. Biophys. Acta 237 (2) (1971) 335–338, https://doi.org/10.1016/0304-4165(71)90327-8.
[15] A.J. Kettle, C.C. Winterbourn, Assays for the chlorination activity of myeloperoxidase, Methods Enzymol. 233 (1994) 502–512, https://doi.org/10.1016/s0076-6879(94)33056-5.
[16] H. Parker, M. Dragunow, M.B. Hampton, A.J. Kettle, C.C. Winterbourn, Requirements for NADPH oxidase and myeloperoxidase in neutrophil extracellular trap formation differ depending on the stimulus, J. Leukoc. Biol. 92 (4) (2012) 841–849, https://doi.org/10.1189/jlb.1211601.
[17] L.J. Palmer, P.R. Cooper, M.R. Ling, H.J. Wright, A. Huissoon, I.L. Chapple, Hypochlorous acid regulates neutrophil extracellular trap release in humans, Clin. Exp. Immunol. 167 (2) (2012) 261–268, https://doi.org/10.1111/j.1365-2249.2011.04518.x.
[18] I. Neeli, S.N. Khan, M. Radic, Histone deimination as a response to inflammatory stimuli in neutrophils, J. Immunol. 180 (3) (2008) 1895–1902, https://doi.org/10.4049/jimmunol.180.3.1895.
[19] O.E. Sørensen, N. Borregaard, Neutrophil extracellular traps - the dark side of neutrophils, J. Clin. Investig. 126 (5) (2016) 1612–1620, https://doi.org/10.1172/jci84538.
[20] H.R. Thiam, S.L. Wong, R. Qiu, M. Kittisopikul, A. Vahabikashi, A.E. Goldman, R. D. Goldman, D.D. Wagner, C.M. Waterman, NETosis proceeds by cytoskeleton and endomembrane disassembly and PAD4-mediated chromatin decondensation and nuclear envelope rupture, Proc. Natl. Acad. Sci. U. S. A. 117 (13) (2020) 7326–7337, https://doi.org/10.1073/pnas.1909546117.
[21] J.R. Yaron, S. Gangaraju, M.Y. Rao, X. Kong, L. Zhang, F. Su, Y. Tian, H.L. Glenn, D. R. Meldrum, K^+ regulates Ca^{2+} to drive inflammasome signaling: dynamic visualization of ion flux in live cells, Cell Death Dis. 6 (10) (2015) e1954, https://doi.org/10.1038/cddis.2015.277.
[22] A. Petretto, M. Bruschi, F. Pratesi, C. Croia, G. Candiano, G. Ghiggeri, P. Migliorini, Neutrophil extracellular traps (NET) induced by different stimuli: a comparative proteomic analysis, PLoS One 14 (7) (2019) e0218946, https://doi.org/10.1371/journal.pone.0218946.
[23] W.D. Williamson, I. Pinto, Histones and genome integrity, Front. Biosci. 17 (3) (2012) 984–995, https://doi.org/10.2741/3969.
[24] G. Millán-Zambrano, A. Burton, A.J. Bannister, R. Schneider, Histone post-translational modifications - cause and consequence of genome function, Nat. Rev. Genet. 23 (9) (2022) 563–580, https://doi.org/10.1038/s41576-022-00468-7.
[25] M.S. Cosgrove, J.D. Boeke, C. Wolberger, Regulated nucleosome mobility and the histone code, Nat. Struct. Mol. Biol. 11 (11) (2004) 1037–1043, https://doi.org/10.1038/nsmb851.
[26] D. Shechter, H.L. Dormann, C.D. Allis, S.B. Hake, Extraction, purification and analysis of histones, Nat. Protoc. 2 (6) (2007) 1445–1457, https://doi.org/10.1038/nprot.2007.202.
[27] T. Kouzarides, Chromatin modifications and their function, Cell 128 (4) (2007) 693–705, https://doi.org/10.1016/j.cell.2007.02.005.
[28] H.J. Hamam, M.A. Khan, N. Palaniyar, Histone acetylation promotes neutrophil extracellular trap formation, Biomolecules 9 (1) (2019) 9010032, https://doi.org/10.3390/biom9010032.
[29] E.A. Chapman, M. Lyon, D. Simpson, D. Mason, R.J. Beynon, R.J. Moots, H. L. Wright, Caught in a Trap? Proteomic analysis of neutrophil extracellular traps in rheumatoid arthritis and systemic lupus erythematosus, Front. Immunol. 10 (2019) 423, https://doi.org/10.3389/fimmu.2019.00423.
[30] L.A.E. Hallberg, N.W. Thorsen, E.A. Hartsema, P.M. Hagglund, C.L. Hawkins, Mapping the modification of histones by the myeloperoxidase-derived oxidant hypochlorous acid (HOCl), Free Radic. Biol. Med. 192 (2022) 152–164, https://doi.org/10.1016/j.freeradbiomed.2022.09.016.
[31] J.I. Kang Jr., J.W. Neidigh, Hypochlorous acid damages histone proteins forming 3-chlorotyrosine and 3,5-dichlorotyrosine, Chem. Res. Toxicol. 21 (5) (2008) 1028–1038, https://doi.org/10.1021/tx7003486.
[32] C.L. Hawkins, Hypochlorous acid-mediated modification of proteins and its consequences, Essays Biochem. 64 (1) (2020) 75–86, https://doi.org/10.1042/EBC20190045.
[33] H. Parker, A.M. Albrett, A.J. Kettle, C.C. Winterbourn, Myeloperoxidase associated with neutrophil extracellular traps is active and mediates bacterial killing in the presence of hydrogen peroxide, J. Leukoc. Biol. 91 (3) (2012) 369–376, https://doi.org/10.1189/jlb.0711387.
[34] E.A. Hartsema, L.A.E. Hallberg, K. Barlous, C.L. Hawkins, Modification of histones by the myeloperoxidase-derived oxidant hypochlorous acid (HOCl) alters their

reactivity with vascular smooth muscle cells, Redox Biochem. Chem. 5–6 (2023) 100010, https://doi.org/10.1016/j.rbc.2023.100010.
[35] M. Moiana, F. Aranda, G. de Larranaga, A focus on the roles of histones in health and diseases, Clin. Biochem. 94 (2021) 12–19, https://doi.org/10.1016/j.clinbiochem.2021.04.019.
[36] T.D. Tsourouktsoglou, A. Warnatsch, M. Ioannou, D. Hoving, Q. Wang, V. Papayannopoulos, Histones, DNA, and citrullination promote neutrophil extracellular trap inflammation by regulating the localization and activation of TLR4, Cell Rep. 31 (5) (2020) 107602, https://doi.org/10.1016/j.celrep.2020.107602.
[37] J.C. Morris, The acid ionization constant of HOCl from 5 °C to 35 °C, J. Phys. Chem. 70 (1966) 3798–3805, https://doi.org/10.1021/j100884a007.
[38] L.A.E. Hallberg, K. Barlous, C.L. Hawkins, Antioxidant strategies to modulate NETosis and the release of neutrophil extracellular traps during chronic inflammation, Antioxidants 12 (2) (2023) 12020478, https://doi.org/10.3390/antiox12020478.
[39] M.B. Pass, N. Borregaard, J.B. Cowland, Derangement of transcription factor profiles during in vitro differentiation of HL60 and NB4 cells, Leuk. Res. 31 (6) (2007) 827–837, https://doi.org/10.1016/j.leukres.2006.07.019.
[40] A.M. Albrett, L.V. Ashby, N. Dickerhof, A.J. Kettle, C.C. Winterbourn, Heterogeneity of hypochlorous acid production in individual neutrophil phagosomes revealed by a rhodamine-based probe, J. Biol. Chem. 293 (40) (2018) 15715–15724, https://doi.org/10.1074/jbc.RA118.004789.
[41] C.S. Hughes, S. Moggridge, T. Müller, P.H. Sorensen, G.B. Morin, J. Krijgsveld, Single-pot, solid-phase-enhanced sample preparation for proteomics experiments, Nat. Protoc. 14 (1) (2019) 68–85, https://doi.org/10.1038/s41596-018-0082-x.
[42] J. Rappsilber, M. Mann, Y. Ishihama, Protocol for micro-purification, enrichment, pre-fractionation and storage of peptides for proteomics using StageTips, Nat. Protoc. 2 (8) (2007) 1896–1906, https://doi.org/10.1038/nprot.2007.261.
[43] Y. Kusunoki, D. Nakazawa, H. Shida, F. Hattanda, A. Miyoshi, S. Masuda, S. Nishio, U. Tomaru, T. Atsumi, A. Ishizu, Peptidylarginine deiminase inhibitor suppresses neutrophil extracellular trap formation and MPO-ANCA production, Front. Immunol. 7 (2016) 227, https://doi.org/10.3389/fimmu.2016.00227.
[44] M. Romana, M. Leduc, P. Hermand, J. Bruce, E.F. Gautier, F. Martino, Y. Garnier, V. Baccini, C. Le Van Kim, Proteomic analysis of neutrophils from patients with COVID-19, Br. J. Haematol. 199 (1) (2022) 61–64, https://doi.org/10.1111/bjh.18347.
[45] H. Tachiwana, W. Kagawa, A. Osakabe, K. Kawaguchi, T. Shiga, Y. Hayashi-Takanaka, H. Kimura, H. Kurumizaka, Structural basis of instability of the nucleosome containing a testis-specific histone variant, human H3T, Proc. Natl. Acad. Sci. U. S. A. 107 (23) (2010) 10454–10459, https://doi.org/10.1073/pnas.1003064107.
[46] C. Skjolberg, L. Degani, I. Sileikaite-Morvakozi, C.L. Hawkins, Oxidative modification of extracellular histones by hypochlorous acid modulates their ability to induce beta-cell dysfunction, Free Radic. Biol. Med. 230 (2025) 209–221, https://doi.org/10.1016/j.freeradbiomed.2025.02.018.
[47] H.R. Thiam, S.L. Wong, D.D. Wagner, C.M. Waterman, Cellular mechanisms of NETosis, Annu. Rev. Cell Dev. Biol. 36 (2020) 191–218, https://doi.org/10.1146/annurev-cellbio-020520-111016.
[48] V. Papayannopoulos, K.D. Metzler, A. Hakkim, A. Zychlinsky, Neutrophil elastase and myeloperoxidase regulate the formation of neutrophil extracellular traps, J. Cell Biol. 191 (3) (2010) 677–691, https://doi.org/10.1083/jcb.201006052.
[49] R.S. Keshari, A. Jyoti, M. Dubey, N. Kothari, M. Kohli, J. Bogra, M.K. Barthwal, M. Dikshit, Cytokines induced neutrophil extracellular traps formation: implication for the inflammatory disease condition, PLoS One 7 (10) (2012) e48111, https://doi.org/10.1371/journal.pone.0048111.
[50] D.M. Williams, A.A. Peden, S-acylation of NLRP3 provides a nigericin sensitive gating mechanism that controls access to the Golgi, eLife 13 (2024) 94302, https://doi.org/10.7554/eLife.94302.
[51] D. Riyapa, D. Rinchai, V. Muangsombut, C. Wuttinontananchai, M. Toufiq, D. Chaussabel, M. Ato, J.M. Blackwell, S. Korbsrisate, Transketolase and vitamin B1 influence on ROS-dependent neutrophil extracellular traps (NETs) formation, PLoS One 14 (8) (2019) e0221016, https://doi.org/10.1371/journal.pone.0221016.
[52] D. Stojkov, L. Gigon, S. Peng, R. Lukowski, P. Ruth, A. Karaulov, A. Rizvanov, N. A. Barlev, S. Yousefi, H.U. Simon, Physiological and pathophysiological roles of metabolic pathways for net formation and other neutrophil functions, Front. Immunol. 13 (2022) 826515, https://doi.org/10.3389/fimmu.2022.826515.
[53] P. Amini, D. Stojkov, A. Felser, C.B. Jackson, C. Courage, A. Schaller, L. Gelman, M. E. Soriano, J.M. Nuoffer, L. Scorrano, C. Benarafa, S. Yousefi, H.U. Simon, Neutrophil extracellular trap formation requires OPA1-dependent glycolytic ATP production, Nat. Commun. 9 (1) (2018) 2958, https://doi.org/10.1038/s41467-018-05387-y.
[54] K. Xie, M. Varatnitskaya, A. Maghnouj, V. Bader, K.F. Winklhofer, S. Hahn, L. I. Leichert, Activation leads to a significant shift in the intracellular redox homeostasis of neutrophil-like cells, Redox Biol. 28 (2020) 101344, https://doi.org/10.1016/j.redox.2019.101344.
[55] X. Chen, B.J. Cuffari, V. Dubljevic, A. Shirali, J. Zhou, J.A. Campbell, S.C. Suits, K. M. O'Sullivan, J.E. Hansen, Inhibition of NETosis by a nuclear-penetrating anti-DNA autoantibody, Immunohorizons 6 (6) (2022) 356–365, https://doi.org/10.4049/immunohorizons.2100091.
[56] S.J. Weiss, R. Klein, A. Slivka, M. Wei, Chlorination of taurine by human-neutrophils - evidence for hypochlorous acid generation, J. Clin. Investig. 70 (3) (1982) 598–607, https://doi.org/10.1172/jci110652.
[57] H. Lin, B.S. Levison, J.A. Buffa, Y. Huang, X. Fu, Z. Wang, V. Gogonea, J. A. DiDonato, S.L. Hazen, Myeloperoxidase-mediated protein lysine oxidation generates 2-aminoadipic acid and lysine nitrile in vivo, Free Radic. Biol. Med. 104 (2017) 20–31, https://doi.org/10.1016/j.freeradbiomed.2017.01.006.
[58] D.I. Pattison, M.J. Davies, Reactions of myeloperoxidase-derived oxidants with biological substrates: gaining chemical insight into human inflammatory diseases, Curr. Med. Chem. 13 (2006) 3271–3290, https://doi.org/10.2174/092986706778773095.
[59] D. Ross, D. Siegel, Functions of NQO1 in cellular protection and coq10 metabolism and its potential role as a redox sensitive molecular switch, Front. Physiol. 8 (2017) 595, https://doi.org/10.3389/fphys.2017.00595.
[60] D.I. Pattison, C.L. Hawkins, M.J. Davies, Hypochlorous acid-mediated protein oxidation: how important are chloramine transfer reactions and protein tertiary structure? Biochemistry 46 (2007) 9853–9864, https://doi.org/10.1021/bi7008294.
[61] Y. Shao, L. Li, L. Liu, Y. Yang, J. Huang, D. Ji, Y. Zhou, Y. Chen, Z. Zhu, B. Sun, CD44/ERM/F-actin complex mediates targeted nuclear degranulation and excessive neutrophil extracellular trap formation during sepsis, J. Cell Mol. Med. 26 (7) (2022) 2089–2103, https://doi.org/10.1111/jcmm.17231.
[62] E. Ramos Caceres, L. Kemperman, K.M. Bonger, Environment-sensitive turn-on fluorescent probe enables live cell imaging of myeloperoxidase activity during NETosis, Commun. Chem. 7 (1) (2024) 262, https://doi.org/10.1038/s42004-024-01338-5.
[63] T.L. Bennike, M. Olesen, V. Andersen, S. Birekelund, A. Stensballe, Optimizing the identification of citrullinated peptides by mass spectrometry: utilizing the inability of trypsin to cleave after citrullinated amino acids, J. Proteonomics Bioinf. 6 (2013) 288–295, https://doi.org/10.4172/jpb.1000293.
[64] D. Zhu, Y. Zhang, S. Wang, Histone citrullination: a new target for tumors, Mol. Cancer 20 (1) (2021) 90, https://doi.org/10.1186/s12943-021-01373-z.
[65] B.N. Gantner, F.R. Palma, C. Kayzuka, R. Lacchini, D.R. Foltz, V. Backman, N. Kelleher, A. Shilatifard, M.G. Bonini, Histone oxidation as a new mechanism of metabolic control over gene expression, Trends Genet. 40 (9) (2024) 739–746, https://doi.org/10.1016/j.tig.2024.05.012.
[66] G.A.F. Nicolaes, O. Soehnlein, Targeting extranuclear histones to alleviate acute and chronic inflammation, Trends Pharmacol. Sci. 45 (7) (2024) 651–662, https://doi.org/10.1016/j.tips.2024.05.008.
[67] P. Szatmary, W. Huang, D. Criddle, A. Tepikin, R. Sutton, Biology, role and therapeutic potential of circulating histones in acute inflammatory disorders, J. Cell Mol. Med. 22 (10) (2018) 4617–4629, https://doi.org/10.1111/jcmm.13797.
[68] E. Silk, H. Zhao, H. Weng, D. Ma, The role of extracellular histone in organ injury, Cell Death Dis. 8 (5) (2017) e2812, https://doi.org/10.1038/cddis.2017.52.
[69] C. Silvestre-Roig, Q. Braster, K. Wichapong, E.Y. Lee, J.M. Teulon, N. Berrebeh, J. Winter, J.M. Adrover, G.S. Santos, A. Froese, P. Lemnitzer, A. Ortega-Gomez, R. Chevre, J. Marschner, A. Schumski, C. Winter, L. Perez-Olivares, C. Pan, N. Paulin, T. Schoufour, H. Hartwig, S. Gonzalez-Ramos, F. Kamp, R.T.A. Megens, K.A. Mowen, M. Gunzer, L. Maegdefessel, T. Hackeng, E. Lutgens, M. Daemen, J. von Blume, H.J. Anders, V.O. Nikolaev, J.L. Pellequer, C. Weber, A. Hidalgo, G. A.F. Nicolaes, G.C.L. Wong, O. Soehnlein, Externalized histone H4 orchestrates chronic inflammation by inducing lytic cell death, Nature 569 (7755) (2019) 236–240, https://doi.org/10.1038/s41586-019-1167-6.
[70] Y. Perez-Riverol, J. Bai, C. Bandla, D. Garcia-Seisdedos, S. Hewapathirana, S. Kamatchinathan, D.J. Kundu, A. Prakash, A. Frericks-Zipper, M. Eisenacher, M. Walzer, S. Wang, A. Brazma, J.A. Vizcaino, The PRIDE database resources in 2022: a hub for mass spectrometry-based proteomics evidences, Nucleic Acids Res. 50 (D1) (2022) D543–D552, https://doi.org/10.1093/nar/gkab1038.